



DALHOUSIE UNIVERSITY

Retrieved from DalSpace, the institutional repository of
Dalhousie University

<http://hdl.handle.net/10222/80511>

Version: Post-print

Publisher's version: Fabris L, Rolick RL, Kurylyk BL, Carey SK. 2020.

Characterization of contrasting flow and thermal regimes in two adjacent
subarctic alpine headwaters in northwest Canada. *Hydrological Processes*,
34(15): 3252-3270. <https://doi.org/10.1002/hyp.13786>

1 **Characterization of contrasting flow and thermal regimes in two**
2 **adjacent subarctic alpine headwaters in northwest Canada**
3

4 This is the accepted version of Fabris et al., 2020, *Hydrological Processes*. The final published
5 version is available at: <https://onlinelibrary.wiley.com/doi/abs/10.1002/hyp.13786>

6 **Authors:**

7 *Luca Fabris¹, Ryan L. Rolick¹, Barret L. Kurylyk^{1,2}, and Sean K. Carey¹*
8

9 **Affiliations:**

10 ¹Watershed Hydrology Group, School of Geography and Earth Sciences, McMaster University, Hamilton, L8S 4L8,
11 Canada

12 ²Centre for Water Resources Studies and Department of Civil and Resource Engineering, Dalhousie University,
13 Halifax, Nova Scotia, Canada

14
15 * Corresponding author: Luca Fabris (fabrisl@mcmaster.ca)
16
17
18

19 **Data Availability Statement**

20 Plots depicting the data that support the findings of this study are available in the supplementary
21 material of this article, while numerical data are available from the corresponding author upon
22 reasonable request.
23

24 **Acknowledgements:**

25 Financial support for this project was provided by the Natural Sciences and Engineering
26 Research Council of Canada (NSERC) through their Discovery Program and the Changing Cold

27 Regions Network (CCRN). Further support was provided by the Global Water Futures (GWF)
28 program under the Canada First Research Excellence Fund. The authors would like to thank
29 Nadine Shatilla, Renée Lemmond and Heather Bonn for help in the field. Logistical and data
30 support of the Water Resources Branch, Department of Environment, Government of Yukon, is
31 gratefully acknowledged.

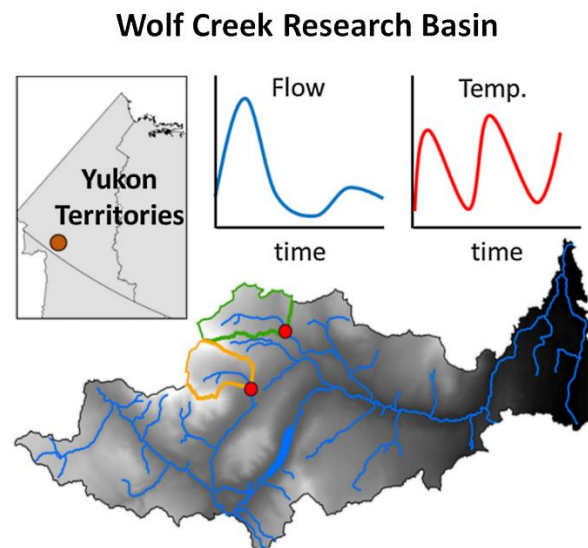
32
33

34 **Key words:** flow regime; stream temperature; heat budget; energy balance; subarctic alpine
35 headwaters; regression analysis; permafrost; climate change

36 **Abstract**

37 Alpine headwaters in subarctic regions are particularly sensitive to climate change, yet there is
38 little information on stream thermal regimes in these areas and how they might respond to global
39 warming. In this paper, we characterize and compare the hydrological and thermal regimes of
40 two subarctic headwater alpine streams within an empirical framework. The streams investigated
41 are located within two adjacent catchments with similar geology, size, elevation and landscape,
42 Granger Creek (GC) and Buckbrush Creek (BB), which are part of the Wolf Creek Research
43 Basin in the Yukon Territory, Canada. Hydrometeorological and high-resolution stream
44 temperature data were collected throughout summer 2016. Both sites exhibited a flow regime
45 typical of cold alpine headwater catchments influenced by frozen ground and permafrost.
46 Comparatively, GC was characterized by a flashier response with more extreme flows, than BB.
47 In both sites, stream temperature was highly variable and very responsive to short-term changes
48 in climatic conditions. On average, stream temperature in BB was slightly higher than in GC
49 (respectively 5.8 °C and 5.7 °C), but less variable (average difference between 75th - 25th
50 quantiles of 1.6 °C and 2.0 °C). Regression analysis between mean daily air and stream

51 temperature suggested that a greater relative (to stream flow) groundwater contribution in BB
52 could more effectively buffer atmospheric fluctuations. Heat fluxes were derived and utilized to
53 assess their relative contribution to the energy balance. Overall, non-advective fluxes followed a
54 daily pattern highly correlated to short-wave radiation. Generally, solar radiation and latent heat
55 were respectively the most important heat source and sink, while air-water interface processes
56 were major factors driving nighttime stream temperature fluctuations.



58 **Graphical abstract**

59 **1 INTRODUCTION**

60 Stream temperature is a key factor regulating chemical, physical and biological processes within
61 rivers (Webb, Hannah, Moore, Brown & Nobilis, 2008), such as the distribution and growth rate
62 of aquatic organisms (Marine & Cech, 2004), concentration of dissolved oxygen and sediments
63 (Ficklin, Stewart & Maurer, 2013), and the release of nutrients (Mcdowell, Elkin & Kleinman,
64 2017). Consequently, riverine ecosystems are very sensitive to alterations of diel and seasonal
65 stream thermal cycles and spatial temperature patterns (Fullerton *et al.*, 2018; Kurylyk *et al.*,
66 2015; Steel *et al.*, 2017). These alterations can be the result of natural changes, anthropogenic

67 perturbations, or their combinations (Caissie, 2006). The main anthropogenic perturbations
68 include deforestation (e.g. Bourque & Pomeroy, 2001), flow modifications (e.g. construction of
69 water reservoirs and canalization, Ferrazzi & Botter, 2019; Gaay & Blokland, 1970; Liu, Yang,
70 Ye & Berezovskaya, 2005), urban water inputs and withdrawals (e.g. Kinouchi, Yagi &
71 Miyamoto, 2007), and climate change (e.g. Ficklin *et al.*, 2013; Isaak, Wollrab, Horan &
72 Chandler, 2012).

73 Presently, climate change represents the most concerning threat for river thermal environments at
74 a global scale, with considerable research directly linking long-term increases in stream
75 temperatures to global warming (e.g. Arora, Tockner & Venohr, 2016; Hari, Livingstone, Siber,
76 Burkhardt-Holm & Guttinger, 2006; Isaak *et al.*, 2012; Mayer, 2012). Stream temperature is the
77 result of complex interactions between heat fluxes at the air-water interface (radiative and
78 turbulent fluxes) (Caissie, 2006; Hebert, Caissie, Satish & El-jabi, 2011; Leach & Moore, 2010),
79 streambed conduction (Caissie & Luce, 2017), and advective processes occurring along the
80 channel with streamflow, across the streambed interface due to groundwater-surface water
81 interactions (Briggs *et al.*, 2018; Caissie & Luce, 2017; Kurylyk, Moore & Macquarrie, 2016), or
82 transversely due to runoff, bank seeps or springs, or tributary inflows (Harrington, Hayashi &
83 Kurylyk, 2017; Leach & Moore, 2014). Climate change will alter the thermal cycle in two
84 distinct ways: directly, by altering the surface energy fluxes, which normally dominate a
85 stream's energy budget; and indirectly, by changing hydrological conditions and thus advective
86 fluxes and thermal inertia (Pekarova, Halmova, Miklanek, Onderka, Pekar & Skoda., 2008;
87 Poole & Berman, 2001; Vliet, Ludwig, Zwolsman, Weedon & Kabat, 2011).

88 The magnitude and temporal patterns of these thermal and hydrologic changes are not uniformly
89 distributed, but are strongly related to nested controls acting at different spatial and temporal

90 scales, including climate (first order), basin characteristics (second order) and reach-specific
91 controls (third order) (Hannah & Garner, 2015; Webb *et al.*, 2008). Understanding how these
92 conditions vary among watersheds may help to explain why some rivers are warming more
93 slowly than others (Isaak *et al.*, 2016; Luce, Staab, Kramer, Wenger, Isaak & McConnell, 2014),
94 and why some river networks or catchments that are historically more thermally resilient are
95 expected to provide future climate refugia and preserve cold-water species (Isaak, Young, Nagel,
96 Horan & Groce, 2015). Therefore, if we wish to improve our capability to predict future patterns
97 and design efficient mitigation and conservation strategies, understanding the hydrological and
98 thermal cycles, and heat fluxes regulating stream temperature in different climatic regions and
99 environmental conditions is fundamental (Macdonald, Boon, Byrne & Silins, 2014).

100 Headwaters are generally characterized by high thermal heterogeneity, low thermal inertia, and
101 variable sources of water inputs (Brown, Hannah & Milner, 2005; Brown & Hannah, 2008;
102 Mayer, 2012; Harrington *et al.*, 2017; Docherty, Abermann, Lund & Hannah, 2019). Of major
103 importance in these streams is the discharge of groundwater (Mayer, 2012), which by acting as a
104 heat source and sink in cold and warm periods respectively, reduces their thermal sensitivity to
105 change in climatic conditions (e.g. air temperature and shortwave radiation) (Evans & Petts,
106 1997; Poole *et al.*, 2008). This results in streams with large groundwater contribution (with
107 respect to longitudinal flow) having reduced temperature variability at multiple time scales (e.g.
108 diel, seasonal) (Kelleher, Wagener, Gooseff, McGlynn, McGuire & Marshall., 2012) , but there is
109 some debate on whether groundwater-dominated systems will also exhibit great resilience to
110 multi-decadal climate warming (Kaandorp, Doornenbal, Kooi, Peter Broers & de Louw, 2019;
111 Kurylyk, MacQuarrie & Voss, 2014). Additionally, the focused discharge of groundwater creates

112 thermal anomalies that provide temporary thermal refugia in both the summer and winter
113 (Power, Brown & Imhof, 1999).

114 Headwater streams in subarctic regions (dominated by permafrost) are particularly susceptible to
115 changes in their thermal regimes, as future climate projections agree that the greatest warming
116 will continue to be observed at both high latitudes and altitudes (Debeer, Wheeler, Carey &
117 Chun, 2016; Pepin *et al.*, 2015). Nevertheless, the bulk of the research has focused on valley
118 bottom rivers (e.g. Broadmeadow, Jones, Langford, Shaw & Nisbet, 2011; Ficklin *et al.*, 2013;
119 Kinouchi *et al.*, 2007) and alpine headwater catchments (e.g. Khamis, Brown, Milner & Hannah,
120 2015; Leach & Moore, 2017; Webb *et al.*, 2008) in temperate regions. Conversely, studies in
121 arctic and subarctic regions are rather rare (e.g. King, Neilson, Overbeck & Kane, 2016; King &
122 Neilson, 2019; Docherty *et al.*, 2019).

123 Another important impact of global warming in cold regions is related to the presence of
124 permafrost and snow accumulated during the cold season. Permafrost is a key control of many
125 hydrological processes such as water storage and connectivity (interaction between shallow and
126 deep subsurface water). The risk of increased permafrost degradation and decreased seasonal
127 ground frost under future climate change (DeBeer *et al.*, 2016; Okkonen, Jyrkama & Kløve,
128 2010) have contributed to an increase of studies conducted on rivers and streams in these regions
129 (e.g. Walvoord and Kurylyk, 2016). Decreases in seasonal or perennial ground ice could
130 potentially lead to more active groundwater systems and deeper routing of subsurface water,
131 causing these systems to gradually exhibit more of the characteristics of groundwater-dominated
132 rivers (Quinton, Hayashi & Chasmer, 2009; Walvoord, Voss & Wellman, 2012).

133 In general, in alpine catchments with snowmelt as the primary source feeding baseflow, an
134 increase in air temperature will alter the timing and duration of snowmelt, increasing the

135 possibility of extremely low flows (Carey, Boucher & Duarte, 2013; MacDonald *et al.* 2014;
136 Okkonen *et al.*, 2010), and thus of extreme water temperatures (Van Vliet, Franssen, Yearsley,
137 Ludwig, Haddeland, Lettenmaier & Kabat, 2013). In contrast, when snowmelt can sustain
138 streamflow throughout the warm season, an increase in air temperature might increase
139 streamflow and reduce its thermal sensitivity to climatic conditions (Lisi, Schindler, Cline,
140 Scheuerell & Walsh, 2015).

141 Hydrological and thermal cycles in cold alpine headwaters in the subarctic region are poorly
142 characterized, but may have critical ecological function under a changing climate (Caissie, 2006;
143 Gooseff, 2010) by providing a ‘cold-water shield’ for at-risk coldwater species (Isaak *et al.*,
144 2015). Accordingly, the overall purpose of this study is to identify the distinctive characteristics
145 of the hydrological and thermal regimes in two adjacent alpine headwaters within the Wolf
146 Creek Research Basin, Yukon Territory (Rasouli, Pomeroy, Janowicz, Williams & Carey, 2019).
147 More specifically the objectives of this paper are to (1) characterize and compare the flow
148 regime dynamics; (2) quantify the relative contribution of different heat fluxes to the stream
149 thermal balance through applying an energy budget approach; and (3) use high-resolution stream
150 temperature data to characterize spatiotemporal thermal patterns.

151 **2 STUDY SITES**

152 Wolf Creek Research Basin (WCRB, 60°32'47" N, 135°11'03" W) is located ~20 km southeast
153 of Whitehorse in Yukon Territory, Canada (Fig. 1a). WCRB has a drainage area of ~179 km²,
154 with elevation ranging between 710 and 2080 m above sea level (a.s.l.). The region is
155 characterized by a subarctic continental climate, with low precipitation and wide air temperature
156 ranges (Rasouli *et al.*, 2019). The average (1981-2010) air temperature measured at the
157 Whitehorse International Airport (706 m a.s.l.) is -0.1 °C, ranging from -15.2 °C (January) to

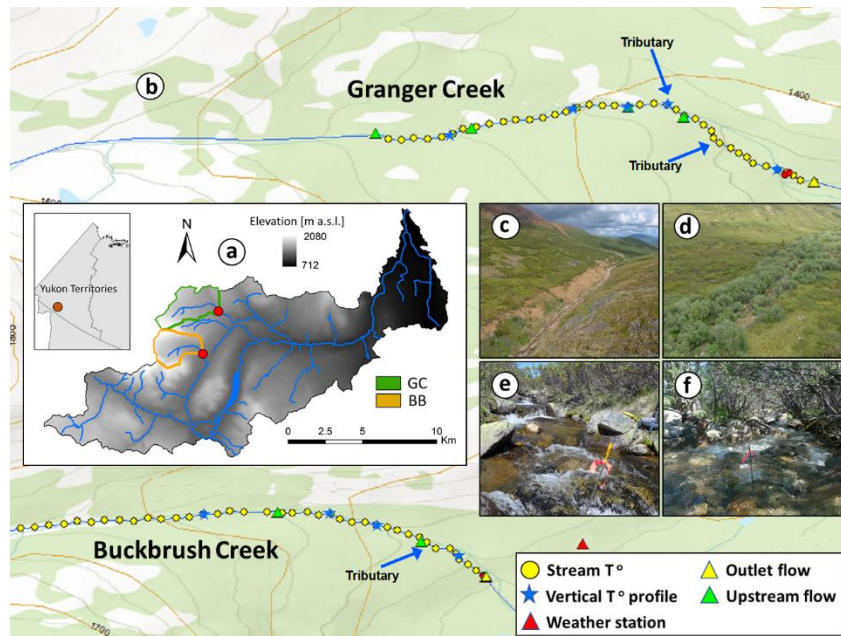
Flow and thermal regimes in subarctic headwaters

158 14.3 °C (July), while average annual precipitation is ~260 mm, of which ~40 % falls as snow.
159 However, due to orographic factors, precipitation in the WCRB at high elevation can be 25 –
160 35 % greater (Pomeroy Hedstrom & Parviainen, 1998).

161 Granger Creek (GC) and Buckbrush Creek (BB) are two headwater catchments located in the
162 northeast of WCRB with similar catchment area (GC: 7.6 km²; BB: 6.1 km²), elevation range
163 (GC: 1355 - 2080 m a.s.l.; BB: 1324 - 2080 m a.s.l.), and main stem flow length (GC: 4.8 km;
164 BB: 3.8 km; Fig. 1a). Each creek has a common west-east flow direction and bed sediment
165 consisting of boulders, cobbles, and gravels, with limited sandy deposits. This study focuses on a
166 1950 m reach of each stream with similar channel characteristics (Fig. 1b). The upper sections of
167 the reaches are relatively narrow, characterized by slightly meandering channels with little
168 shading from vegetation (Fig. 1c and 1d for GC and BB, respectively). Conversely, the lower
169 portions are wider, with a step-pool morphology and denser bank vegetation (Fig. 1e and 1f for
170 GC and BB, respectively). One and two tributaries are present in the lower parts of BB and GC,
171 respectively (blue arrows, Fig. 1b).

172

Flow and thermal regimes in subarctic headwaters



173

174 Fig. 1. Wolf Creek Research Basin (WCRB), Granger Creek (GC) and Buckbrush Creek (BB)
175 basins and their locations (a). Study reaches and gauging stations (b). GC upstream (c) and
176 downstream (e) segments. BB upstream (d) and downstream (f) segments.

177 The geology of these headwater catchments is predominantly sedimentary, and includes

178 limestone, siltstone, sandstone, and conglomerate, overlaid by till (Mougeot and Smith, 1994).

179 Permafrost underlies much of the north-facing aspects, while seasonal frost is dominant in the
180 south-facing slopes and at lower elevations (Carey & Quinton 2005; Lewkowicz & Ednie, 2004).

181 Groundwater discharge has been identified as the main source feeding creeks in the alpine zone
182 using both geophysics (Seguin, Stein, Nilo & Jalbert, 1999) and tracer data (Carey *et al.*, 2013).

183 Vegetation varies with elevation, with tall shrubs (*Salix*) dominating in valley bottoms that
184 transitions to shorter shrubs (*Salix* and *Betula*) as elevation increases, with tundra foliage and
185 bare rock at the highest elevations.

186 **3 METHODOLOGY**

187 **3.1 Field data**

188 The study period spanned the summer field season from 22 June (after snowmelt occurred) to 15
189 September, 2016. Water temperatures were recorded at a 15-minute frequency using iButtons
190 (model iBWetLand DS1922L, precision of ± 0.5 °C, resolution of 0.0625 °C). The loggers were
191 partially shielded in durable silicone and calibrated to 0 °C in a continuously stirred ice bath. In
192 total, 40 calibrated iButtons were used in each stream, with one installed centre-channel on the
193 bed every 50 m along the length of each 1950 m study reach (yellow points, Fig. 1b). Vertically
194 spaced streambed temperature time-series were recorded at a 30-minute frequency at depths of
195 0.05 m and 0.15 m below the sediment-water interface by mounting iButtons in survey stakes
196 and driving them into the bed at various locations in each stream (5 in GC and 4 in BB
197 respectively; blue stars, Fig. 1b) to investigate streambed heat fluxes.

198 Hydrometric stations were established along the length of each creek (5 in GC, 3 in BB),
199 instrumented with Solinst LTC Levelogger Edge pressure transducers to measure stage at 15-
200 minute frequencies (green and yellow triangles, Fig. 1b). Under various flow conditions, water
201 depth and velocity were sampled and utilized to develop stage-discharge relationships for each
202 station according to the velocity-area method (Le Coz, Camenen, Peyrard & Dramais, 2012).
203 Velocity measurements were taken using a SonTek FlowTracker handheld Acoustic Doppler
204 Velocimeter (accuracy $\pm 1\%$) at 0.6 of water depths (0.6-depth method is widely accepted as
205 representative of mean column velocity (Genç, Ardiçlıoğlu & Ağırlioğlu, 2015)). For this
206 analysis, we utilized only flow time series estimated at the stream outlets where more accurate
207 rating curves have been built.

208 Leaf Area Index (LAI) was measured at each sensor location in July using a LI-COR Plant
209 Canopy Analyzer (LAI – 2200C), and upward facing photos were taken with a GoPro Hero3
210 camera to estimate shading factors (SF). A Matlab code was then developed and applied to these
211 photos to estimate the percentage of the frames covered by canopy. Shading factor was
212 considered to vary spatially but be constant in time.

213 Meteorological data were collected at a long-term weather station located near BB (red triangle,
214 Fig. 1b). Along with other parameters, the station measured incoming and outgoing shortwave
215 and longwave radiation (Kipp & Zonen, CNR4), relative humidity, air temperature (Campbell
216 Scientific, HMP45C-L), and wind speed (RM Young) at 30-minute intervals. Evapotranspiration
217 (ET) was measured directly using a LI-7500A (Li-Cor) open path infra-red gas analyzer and a
218 three-axis sonic anemometer (R3-50, Windmaster, Gill Instruments) using standard flux
219 protocols (Baldocchi, Hincks & Meyers, 1988). Precipitation was recorded at 30-minute intervals
220 using a tipping-bucket rain gauge (CS700, Campbell Scientific) located nearby the Buckbrush
221 weather station. Some of the main observations used in this study are shown in the supporting
222 material, (Fig. S1).

223 **3.2 Data analysis**

224 *3.2.1 Flow characterization*

225 For both streams, flow, rainfall and ET measurements were aggregated at hourly and daily time
226 scales. To allow for comparisons between sites and cross-sections, we considered specific
227 discharge (discharge normalized to basin area, q [mm d^{-1}]). Hourly flows were utilized to
228 construct time series and frequency distributions, while daily discharge, precipitation, and ET
229 were used to derive cumulative frequencies and to estimate water deficits. Overall, these
230 provided a robust base from which to analyze flow patterns and form inter-site comparisons.

231 3.2.2 Energy budget

232 Stream temperature patterns are the result of the spatiotemporal variability in the energy
 233 available to the stream through advective and non-advective processes. The total energy
 234 available (Q_n) can be estimated as (Khamis *et al.*, 2015; Webb & Zhang, 1997):

235
$$Q_n = \Phi_{SW} + \Phi_{LW} + \Phi_{lat} + \Phi_{sens} + \Phi_{bed} + \Phi_{fric} + Q_{adv} \quad (1)$$

236 where Φ_{SW} , the net shortwave radiation, is the energy coming directly from the sun (measured)
 237 reduced by reflection and shading (Glose, Lautz, Baker, 2017), and Φ_{LW} is the net longwave
 238 radiation, determined as the sum of two different contributions: longwave emitted from the
 239 atmosphere and landcover (Φ_{Lin}), and emitted longwave radiations at the stream surface (Φ_{emit}).
 240 These were either measured or estimated according to the commonly used Stefan-Boltzmann law
 241 (Glose *et al.*, 2017). The latent heat, Φ_{lat} , is the energy used for either condensation or
 242 evaporation estimated as a function of water temperature, wind speed and vapour pressure
 243 (Evans, McGregor & Petts, 1998; Webb and Zhang, 1997); Φ_{sens} , the sensible heat, is the transfer
 244 of energy between air and the stream surface and was calculated multiplying Φ_{lat} by the Bowen
 245 ratio (Garner, Malcolm, Sadler & Hannah, 2017); Φ_{bed} , the streambed conduction, is the heat
 246 transferred between the streambed and water calculated via Fourier's law using a shallow
 247 streambed temperature logger (Moore, Sutherland, Gomi & Dhakal, 2005b); Φ_{fric} , frictional heat,
 248 is the energy gained from the water as consequence of the friction against riverbed, estimated
 249 according to Theurer, Voos and Miller (1984). This approach provides a potential (maximum)
 250 value, as it considers that all of the potential elevation energy is converted into streambed
 251 friction. Finally, Q_{adv} represents the combined fluxes due to lateral or longitudinal advection. For
 252 our purposes, Q_{adv} is a lumped, unmeasured term whose cumulative effects on stream
 253 temperature are equivalent to the thermal influence of combined advective fluxes. We consider it

254 only qualitatively and relative to the non advective fluxes ($Q_{nadv} = Q_n - Q_{adv}$). For example, if
255 stream temperature in a cross section is constant, Q_{nadv} must have the same magnitude of Q_{adv} but
256 opposite sign. The supplementary material presents a more detailed description of the methods
257 and equations utilized to estimate the heat fluxes. Hourly time series of non-advective fluxes
258 were then derived and utilized to identify diel patterns.

259 *3.2.3 Stream temperature patterns*

260 Stream temperature time series were utilized to create stream temperature maps and boxplots,
261 and to identify spatial and temporal patterns. Boxplots, providing a graphical representation of
262 the main statistics of stream temperature distribution, allowed quantitative comparisons between
263 different reaches and along the same reach. We considered sections 150 m apart and made a
264 distinction between the warmer and cooler periods, early (June 22nd to August 26th) and late
265 (August 27th to September 15th) summer, respectively.

266 *3.2.4 Relationships between stream temperature and thermal processes*

267 Linear regressions between mean daily air and water temperature were derived and used to
268 investigate the relative impact of atmospheric thermal controls vs. other influences, and to
269 quantify the ‘stream thermal sensitivity from regression slopes and intercepts (Caissie, 2006;
270 Kelleher *et al.*, 2012; Mayer, 2012). For example, streams dominated by advective
271 (groundwater) fluxes are generally characterized by lower slopes and higher intercepts, while
272 non-groundwater dominated catchments have higher slopes and intercepts closer to the origin
273 (Caissie, 2006). Regression plots were derived both for entire reaches and for single sections.
274 Lag frequency distributions were utilized to qualitatively evaluate the importance of advective
275 and non-advective fluxes on daily stream temperature maxima. We considered the difference
276 between peaking time of air and stream temperatures ($\text{Lag } T_{stream} - T_{air}$), and non-advective fluxes

277 and stream temperature ($\text{Lag } T_{\text{stream}} - Q_{\text{adv}}$) using hourly time steps. As peaking time depends
278 also on upstream conditions, for each reach we considered stream temperature at the outlet as
279 this represents an aggregate value for the entire reach. We hypothesize that temperature in
280 streams more influenced by atmospheric conditions will closely follow air temperature and non
281 advective fluxes and thereby exhibit a short lag, while those characterized by strong thermal
282 influence from groundwater or other inflows will exhibit longer lags.

283 Finally, to complete our characterization of stream temperature dynamics in subarctic
284 headwaters, we investigated the key drivers regulating overnight stream temperature, when
285 shortwave radiation is not an important factor. In particular, we assessed the influence of air-
286 water and bed-water interface processes, stream temperature, and discharge on nighttime stream
287 temperature variations. For each component, coefficients of determination (R^2) were evaluated at
288 each location. Air temperature was used as a proxy for air-water interface processes, while bed-
289 water interface processes were derived as the sum of overnight conduction and friction fluxes.
290 Nighttime was taken as 10 pm to 4 am when shortwave radiation input was near zero.

291 **4 RESULTS**

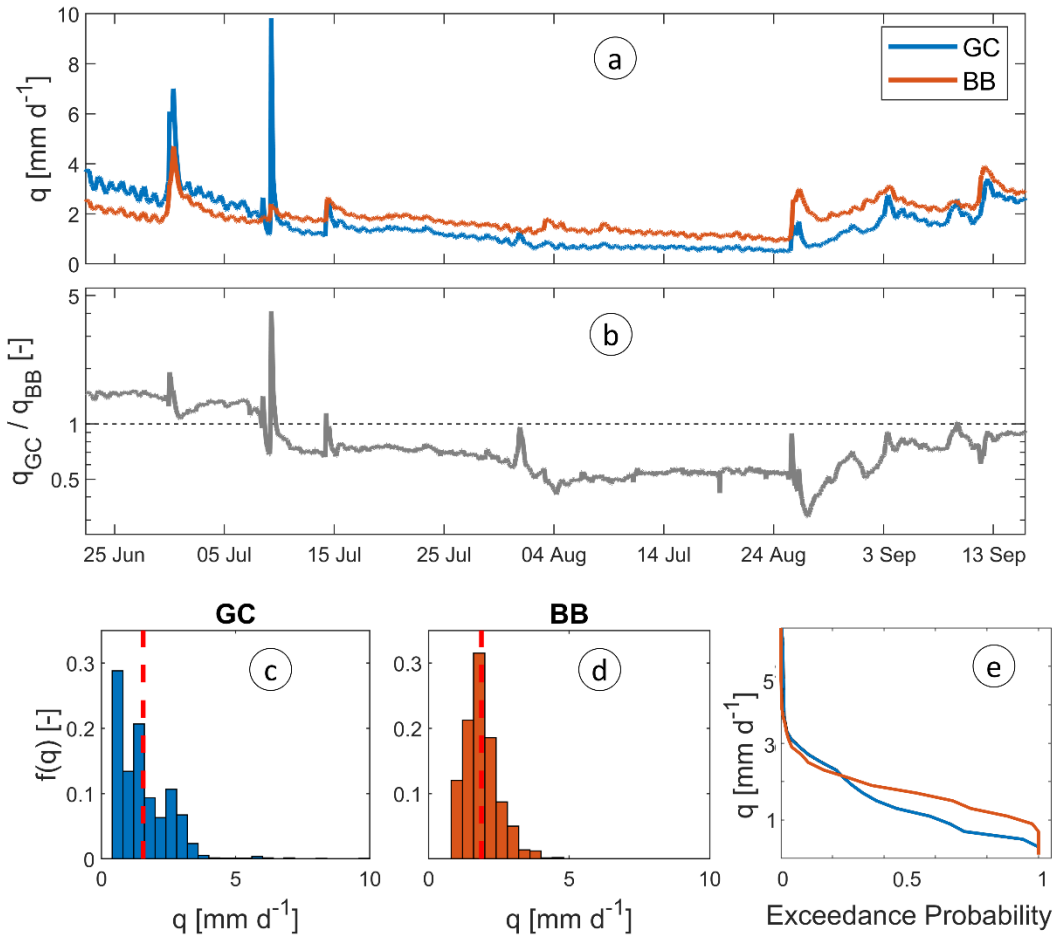
292 For the June – September 2016 study period, 187.4 mm of rain fell compared with a long-term
293 average of 199 mm as measured at the BB weather station (Rasouli et al., 2019). The average
294 temperature over this period was 9°C, approximately 2.5°C cooler than the long-term average,
295 with all months having below normal values.

296 ***4.1 Stream hydrographs***

297 The mean discharges for the study period (22 June – 15 September 2016) at the reach outlets of
298 BB and GC were approximately equal at 1.6 and 1.9 mm d⁻¹ (both ~0.13 m³ s⁻¹), respectively.

Flow and thermal regimes in subarctic headwaters

299 Overall, the two headwaters exhibited similar temporal patterns in the hydrographs ($r = 0.74$),
300 with a strong response to early season precipitation when the active layer was thin and frozen
301 soils widespread, a moderate response in the middle of the summer when conditions were
302 warmer and drier, and an increase in flow at the end of the season when precipitation increased
303 and ET was low (Fig. 2a). Although flow patterns showed common features, significant
304 differences were identified. GC exhibited a flashier response with greater variability (coefficient
305 of variation, CV equal to 0.61 and 0.31 in GC and BB respectively) between wet and dry periods
306 (peaks $>6.0 \text{ mm d}^{-1}$, alternating to low baseflow $<0.6 \text{ mm d}^{-1}$) than BB, which was characterized
307 by a more persistent and stable flow (peaks $<3.5 \text{ mm d}^{-1}$, baseflow $>0.9 \text{ mm d}^{-1}$; Fig. 2a, 2c). The
308 ratio between the specific discharges in GC and BB generally ranged between 0.5 and 1.5 (Fig.
309 2b). Early in the season, specific discharge in GC was much higher than in BB (ratio >1). In the
310 middle of the summer (the driest period), around 12 July, this pattern switched, with BB having
311 higher specific flow than GC (ratio <1). Towards the end of the season, the ratio progressively
312 moved towards 1.

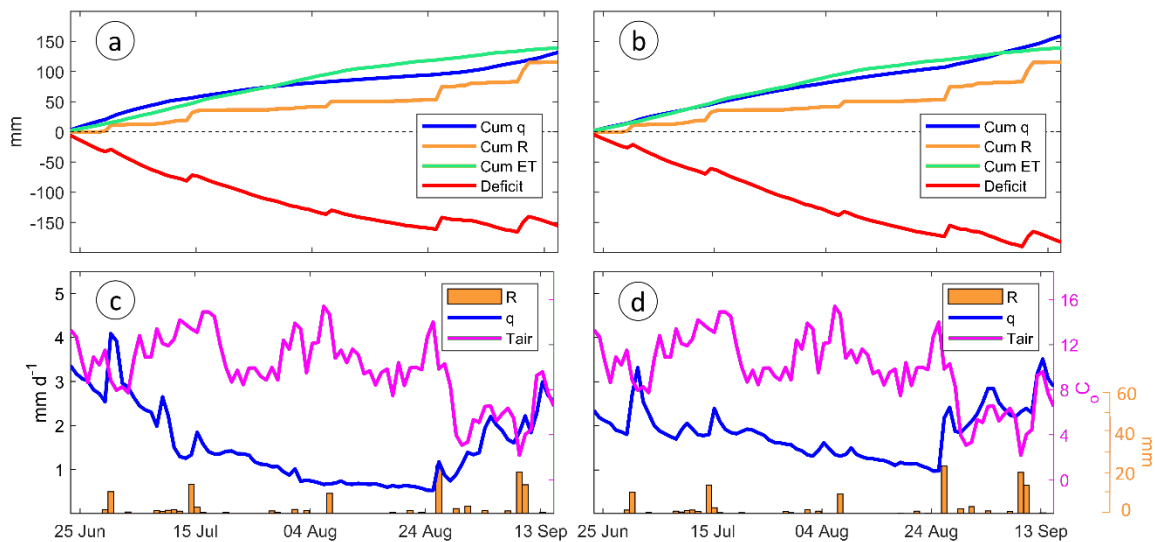


313 Fig. 2. GC and BB specific flow time series (a) and specific flow ratio (b, logarithmic scale). The
 314 highest divergence between the two sites occurred on 9 July when a major flood was recorded in
 315 GC but not in BB. Specific flow frequency distribution (interval = 0.4 mm d-1) in GC (c) and
 316 BB (d), and their exceedance probability curves (e). Red dashed line indicates the mean
 317 discharge.
 318

319
 320 The two sites also showed contrasting specific discharge frequency distributions. In BB, the
 321 discharge was more regular (CV = 0.31) and the distribution less skewed, with flows closer to the
 322 mean (Fig. 2d). Conversely, GC was characterized by a more erratic flow regime with enhanced
 323 intra-seasonal streamflow variability (CV = 0.50; Fig. 2c).

324 Fig. 3 a-b show the cumulative runoff (q), rain (R), evapotranspiration (ET), and deficit (P - (q +
 325 ET)) in GC and BB, respectively. Within the period considered, the loss of water is evenly
 326 divided between q and ET (average q/ET ratio ~1.04). In both sites, until late August (Fig. 3 c-d),

327 precipitation was not sufficient to compensate for water losses from q and ET . As a result, this
 328 period was characterized by increasing water deficit and decreasing baseflow (Fig. 3 a-b). This
 329 highlights the key role played by snowmelt and groundwater storage in sustaining summer
 330 baseflow. In the latest part of the season, only when R increased and ET decreased (due to a
 331 sudden drop in air temperature and declines in available energy, Fig. 3 c-d), the water deficit
 332 stabilized and flow progressively increased.



333 Fig. 3. Cumulative specific flow (q), rainfall (R), evapotranspiration (ET), and deficit ($P - (q +$
 334 $ET)$), for GC (a) and BB (b). Daily time series of flow, air temperature, and amount of
 335 precipitation in GC (c) and BB (d).
 336
 337

338 4.2 Non-advective heat fluxes

339 Figs. 4-6 show different aspects of non-advective fluxes in GC and BB. The contributions of
 340 these fluxes were not constant and varied significantly both in time and space (between reaches
 341 and sections within the same reach; Figs. 5-6). Overall, there is a clear diel pattern for all the
 342 fluxes but the friction flux, whose variability in time is mainly discharge driven (Fig. 4a).

343 Net shortwave radiation (Φ_{SW}) was the primary mechanism of energy gain in both early and late
 344 summer (Fig. 4 b-c, Fig. 6). Hourly averaged Φ_{SW} showed very high correlation (~ 0.97) with net
 345

346 non-advective flux (Q_{nadv} ; Fig. 4a). The magnitude and variability of Φ_{sw} significantly decreased
347 in the last part of the season (Fig. 4 b-c). Medians decreased from ~ 104 to ~ 18 $W\ m^{-2}$, while the
348 difference between the 3rd and the 1st quantiles was reduced by ~ 60 % (from ~ 309 to ~ 121 $W\ m^{-2}$).
349 Φ_{sw} ranged from 44 to 74 % of the total incoming flux (Fig. 5). Spatial
350 variability was mainly driven by differences in shading (SF).

351 The second most important positive contribution was the (potential) bed friction flux (Φ_{fric} ; Fig.
352 6) with a median of ~ 32 and ~ 47 $W\ m^{-2}$ in early and late summer respectively (Fig. 4 b-c). The
353 relative contribution of Φ_{fric} was higher in wetter periods (first and last part of the season; Fig. 6).
354 Peaks of more than 40 % were reached at the end of the season when air temperature and
355 shortwave radiation intensity were lower. Moving downstream, the relative contribution of Φ_{fric}
356 tended to increase with discharge, as expected given the standard formulation (Theurer *et al.*,
357 1984).

358 Overall, net longwave radiation (Φ_{LW}) provided a negligible positive contribution, as
359 atmospheric and emitted longwave radiations had similar magnitude but opposite signs and
360 tended to offset each other (Fig. 4a). More specifically, the contribution of Φ_{LW} was positive
361 during the warmer part of the season (median ~ 7 $W\ m^{-2}$, Fig. 4b), and negative from late August
362 onward (median ~ -7 $W\ m^{-2}$, Fig. 4c) when air temperature could account for up to 40 % of the
363 total negative flux (Fig. 6).

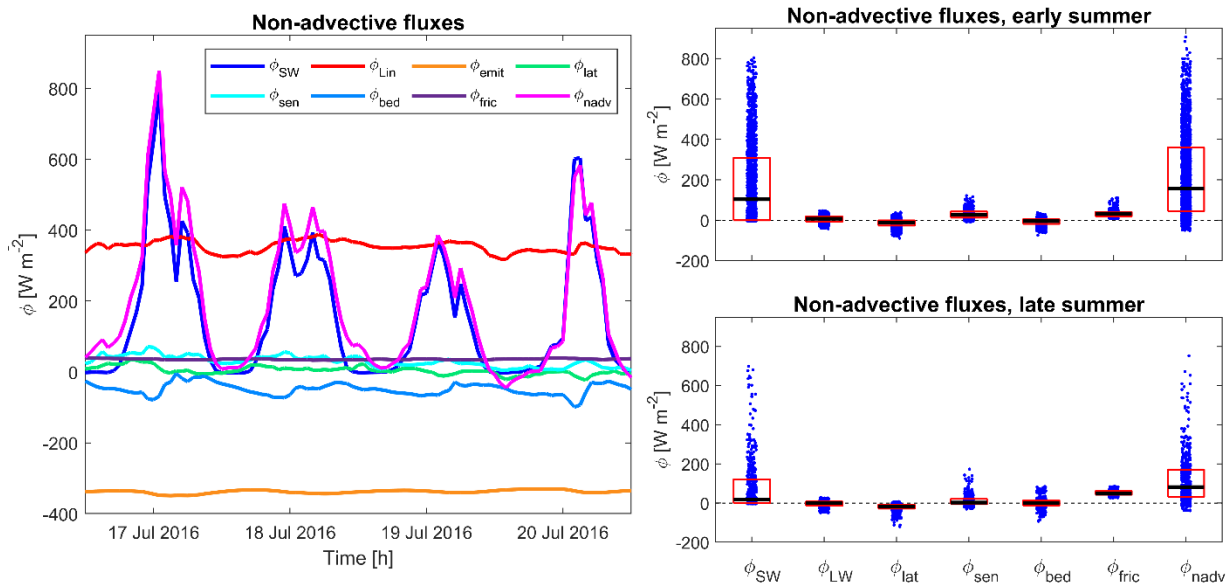
364 Among non-advective fluxes, latent heat exchange (Φ_{lat}) was the dominant process by which heat
365 was lost during the study period, with an average median of ~ -10 $W\ m^{-2}$ (Fig. 4b-c). Its relative
366 contribution to negative Q_{nadv} ranged between 33 and 100 % (Fig. 6).

367 Sensible heat flux (Φ_{sens}) was negative only for a few days, around 15 July in BB. Its
368 contribution was significant in early summer (median ~ 27 $W\ m^{-2}$), and negligible in the late

369 season (median $\sim 2 \text{ W m}^{-2}$; Fig. 4 b-c, Fig. 6). The relative contribution of Φ_{sens} did not exhibit
 370 relevant spatial fluctuations in GC or BB (Fig. 5)

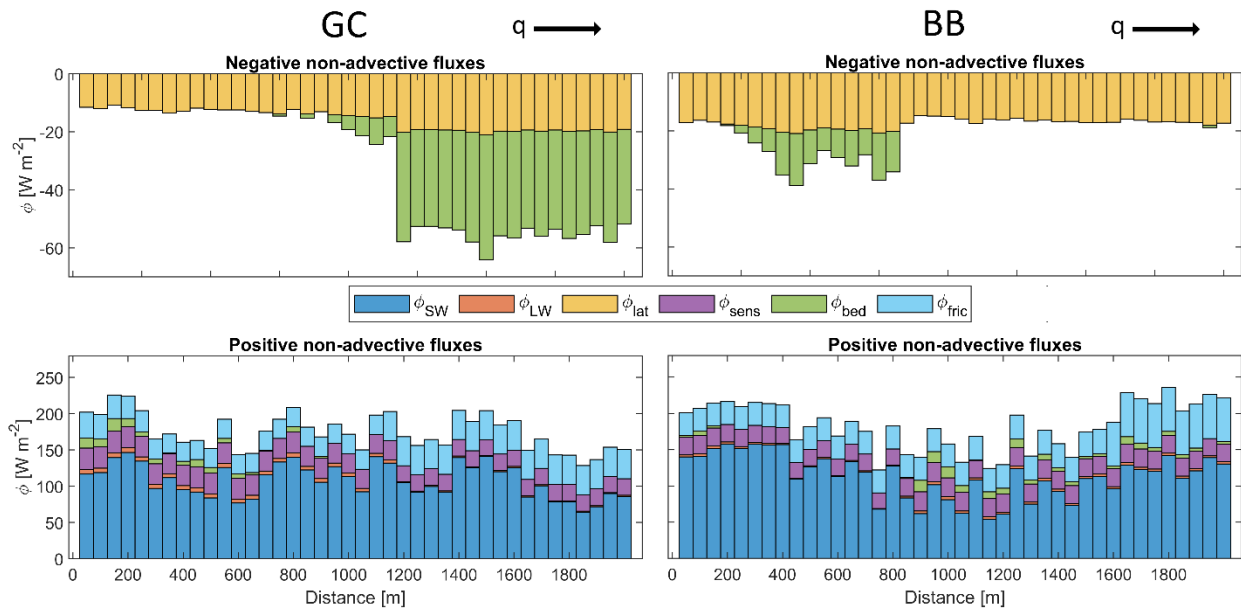
371 Overall, bed conduction (Φ_{bed}) provided negative and positive contributions in early and late
 372 summer, respectively (median ~ -4 and $\sim 1 \text{ W m}^{-2}$; Fig. 4 b-c). Φ_{bed} was the second most
 373 important negative flux (Fig. 6) and the only flux that changed the sign of its contributions along
 374 the channel length, with the two streams showing specular patterns. In GC (BB) the flux was
 375 positive (negative) in the upper part and negative (positive) in the lower part of the reach (Fig.
 376 5).

377 During daylight hours Q_{nadv} was always positive, but overnight its contribution could be either
 378 negative or positive (Fig. 4a). Average overnight Q_{nadv} was mainly controlled by air temperature,
 379 and thus by Φ_{LW} , Φ_{lat} and Φ_{lat} (R^2 respectively 0.37, 0.37, and 0.32; values averaged across
 380 reaches and sections).



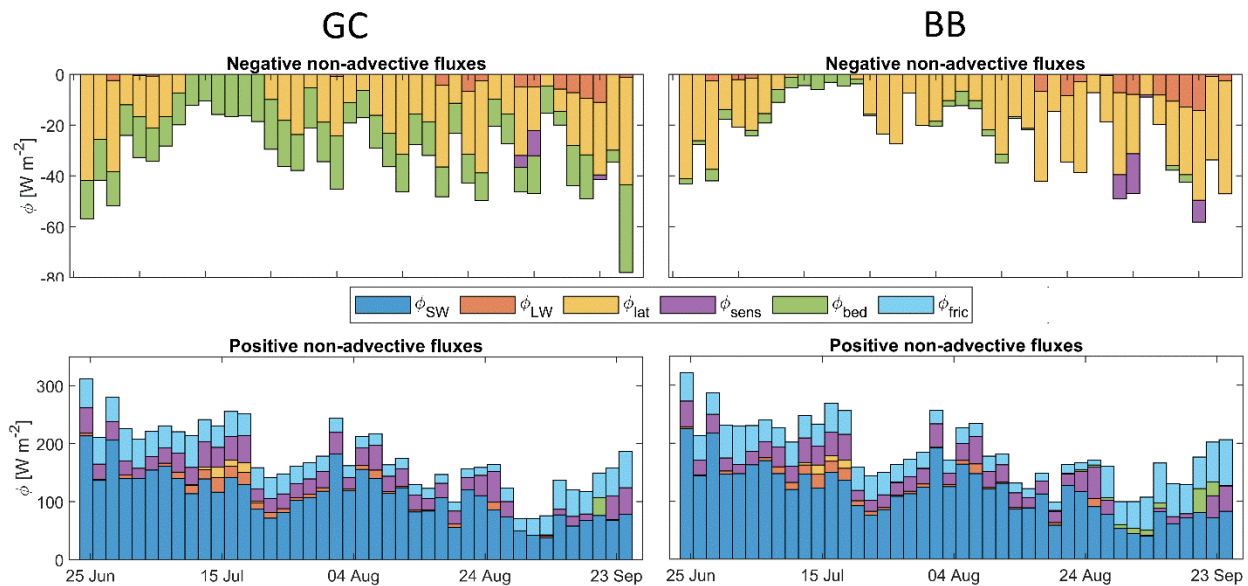
381
 382 Fig. 4. Example of the multi-diel pattern of average (between GC and BB outlets) non-advective
 383 fluxes for a three-day period (a), and boxplots depicting the main statistic of the average
 384 (between sections and reaches) non-advective fluxes for early (22 June to 26 August, b) and late
 385 (27 August to 15 September, c) summer.

386



387
388
389
390
391
392

Fig. 5. For the two streams investigated, overall (averaged over the full study period) non-advective negative fluxes and positive fluxes (below) vs. distance downstream from the upstream station. Atmospheric observations did not vary spatially and for each stream an average streambed temperature was considered. Each bar corresponds to a temperature monitoring station.



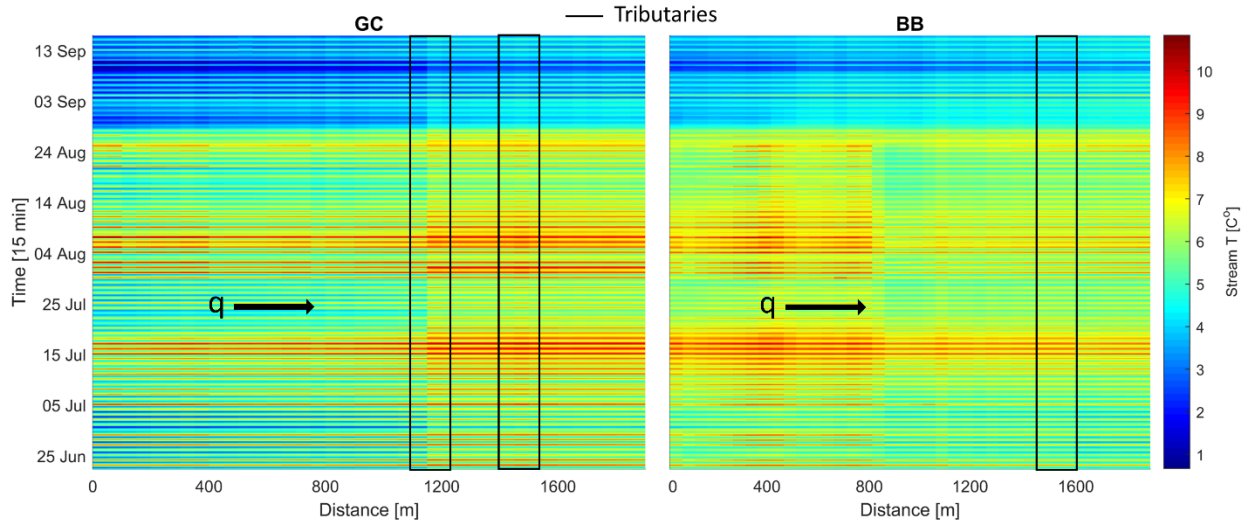
393
394
395
396
397
398
399

Fig. 6. Average (over all stream locations) non-advective negative and positive fluxes (below) vs. time for each of the two streams investigated. Fluxes were estimated at each stream temperature monitoring location. Atmospheric observations did not vary spatially, and for each stream an average streambed temperature was considered. Each bar corresponds to a 2-day interval.

400 **4.3 Thermal regimes**

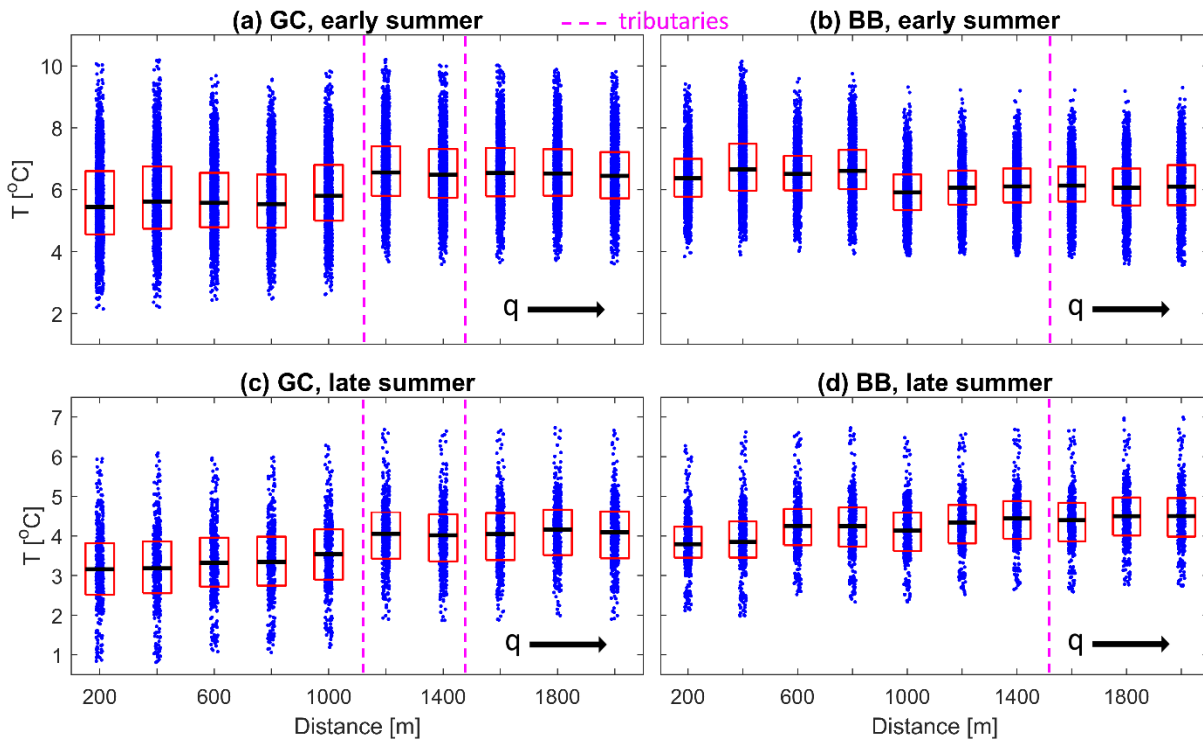
401 The observations captured both the warming and cooling periods over the summer season (Fig.
402 7). Stream temperature showed significant variability both in space and time at different scales.
403 For the measurement period, average summer stream temperature in the two streams was $\sim 3^{\circ}\text{C}$
404 lower than average air temperature (9.0°C). Stream temperature was slightly higher, but less
405 variable in BB (mean 5.8°C , average difference between 75th - 25th quantiles of 1.6°C) than in
406 GC (5.7°C , 2°C) (Fig. 8). For both sites, there was a decrease in stream temperature and
407 variability between early and late summer, with an average median temperature decreasing
408 2.3°C (from 6.0 to 3.7°C) and 2.0°C (from 6.2 to 4.2°C) in GC (Fig. 8 a-c) and BB (Fig. 8 b-
409 d), respectively. Generally, median stream temperature increased with distance downstream (Fig.
410 8); with the exception of BB in early summer, where medians were higher in the upper part of
411 the reach (Fig. 8b). The upper tributary in GC (at 1150 m) was the only tributary significantly
412 affecting stream temperature, with an average difference of $\sim 0.6^{\circ}\text{C}$ between sections upstream
413 and downstream of the confluence (Figs. 7-8). In early summer, it increased downstream
414 temperatures, causing a reduction in variability (spread of blue dots in Fig. 8a), while in late
415 summer, it decreased downstream temperatures without affecting variability (spread of blue dots
416 in Fig. 8c).

Flow and thermal regimes in subarctic headwaters



417
418
419
420
421

Fig. 7. Heat maps representing stream temperature observations in GC and BB reaches. Spatial and temporal resolutions are 50 m and 15 minutes. Black rectangles indicate the position of tributaries.

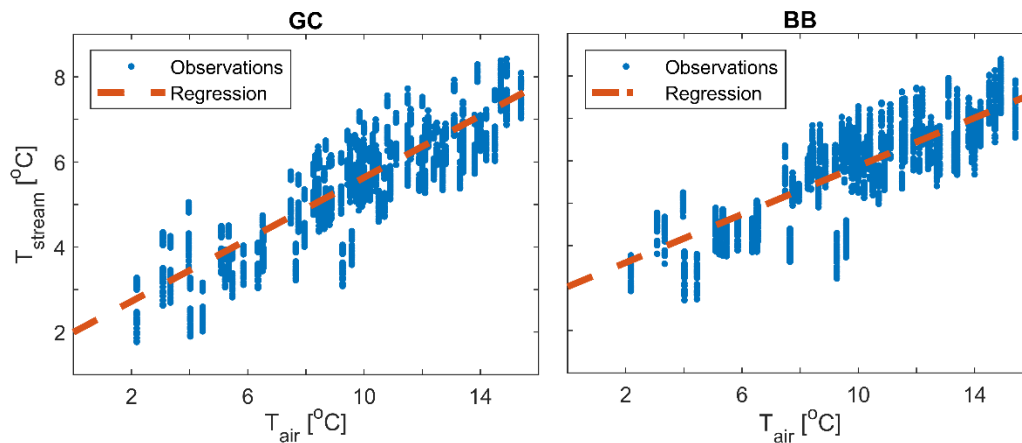


422

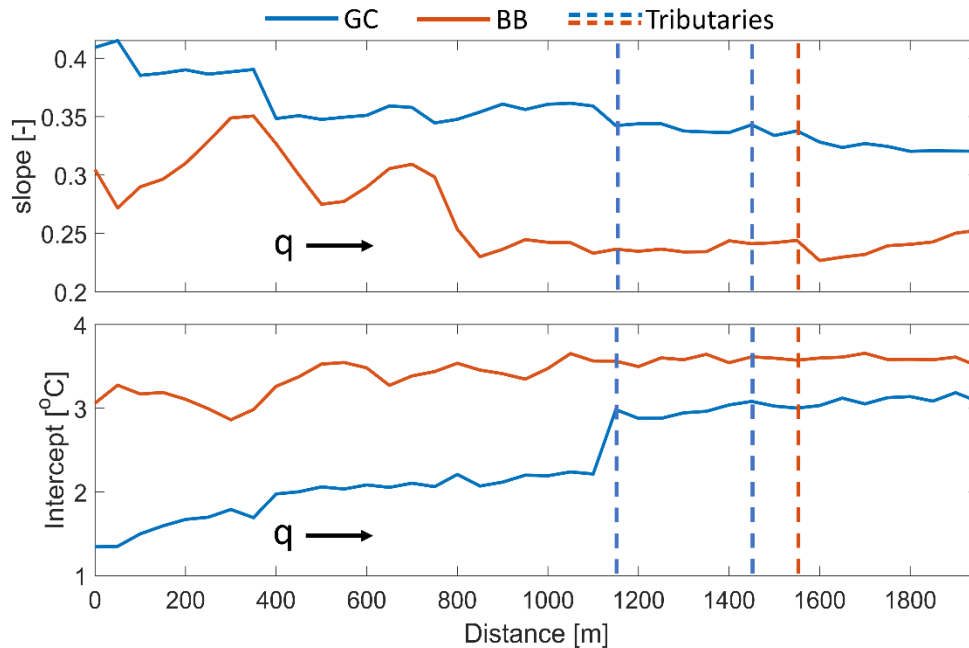
423 Fig. 8. Boxplots depicting some of the main statistics (medians and 25th and 75th quantiles) of
424 temperature observations, early (22 June to 26 August) and late (27 August to 15 September)
425 summer respectively, in GC (a, c) and BB (b, d). Blue dots represent single observations.
426 Sections considered are 200 m apart.
427

428 **4.4 Key controls on daily and sub-daily stream temperatures**

429 Results from the regression analyses between mean daily air and stream temperature for the
 430 entire reaches yielded intercepts of 2.00 and 3.03 °C, and slopes (thermal sensitivities, Kelleher
 431 *et al.*, 2012) of 0.36 and 0.28 (both with a Newey-West Standard Error of ~0.022) in GC and BB,
 432 respectively (Fig. 9), suggesting a greater thermal influence of groundwater in BB than in GC.
 433 However, the slope and intercept were highly variable along the reaches of each stream (Fig. 10).
 434 In GC (BB) the slope ranged between 0.35 and 0.4 (0.22 and 0.39), with its standard error
 435 varying between 0.018 and 0.021 (0.017 and 0.025), while the intercept varied from 1.16 to
 436 2.61 °C (2.13 to 3.56 °C). For both sites, the intercept followed an upward trend downstream.
 437 The slope in BB generally decreased moving downstream, while in GC, there was no clear
 438 spatial pattern.



439 Fig. 9. GC (left) and BB (right), air vs. stream mean daily temperature and corresponding
 440 regression lines. All reach observations were included. The Newey-West Standard Error for the
 441 regression parameter are 0.0222 and 0.0224 for GC and BB.
 442
 443

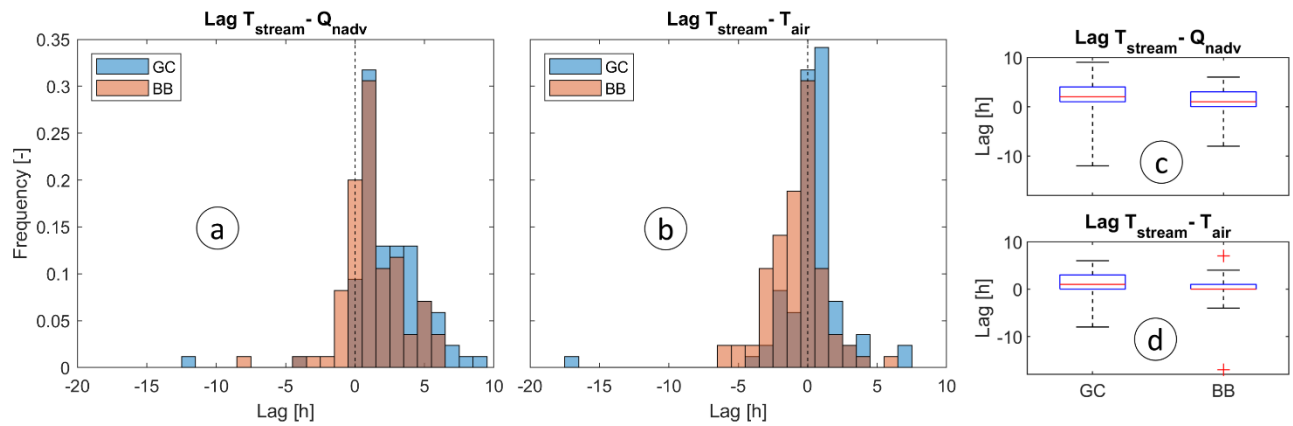


444 Fig. 10. Spatial variability of slope (upper) and intercept (lower) for linear regressions (mean
 445 daily air vs. stream temperatures) in GC and BB. Standard error of the regression parameter
 446 ranges between 0.018 - 0.021 in GC, and 0.017 - 0.025 in BB.
 447
 448

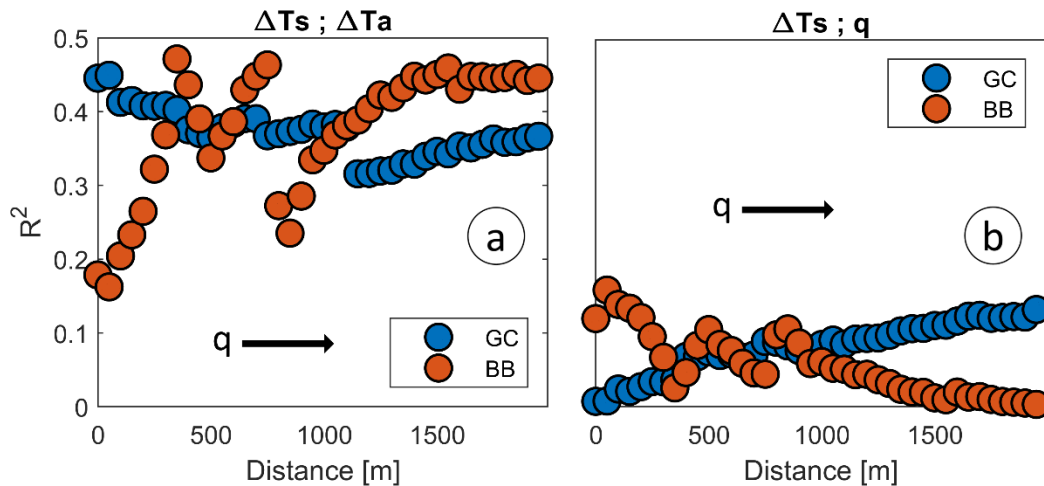
449 In both reaches, $Lag Q_{nadv}-T_{stream}$ (average median equal to 1.5 h) was generally characterized by
 450 more positive values than $Lag T_{air}-T_{stream}$ (average median equal to -0.5 h) (Fig. 11) as air
 451 temperature generally peaked 2 h after the non-advective flux (which as previously shown, was
 452 highly correlated to shortwave radiation). The 2 h delay was consistent in both sites.

453 Daily stream temperatures typically peaked later in GC than in BB. Negative values of the Lag
 454 $Q_{nadv}-T_{stream}$ were unexpected for the summer season and, to our knowledge, are not reported
 455 elsewhere. The reasons for the slightly negative values (>-5 h) were: 1) the stream temperature,
 456 on a given day, did not exhibit a clear peak but a plateau where measurement errors and
 457 approximation might affect the timing of max Q_{nadv} ; 2) the Q_{nadv} could be subject to strong, short
 458 time-scale fluctuations (e.g. due to variability in sky cover), and stream temperature peaks could
 459 occur at persistent high Q_{nadv} that did not coincide with or follow the air temperature daily peak.
 460 Alternatively, larger negative values <-7 h occurred when the overall energy balance was

461 negative throughout the day, as Q_{nadv} (in those days average peak $\sim 165 \text{ W m}^2$) was not sufficient
 462 to compensate advective (negative, according to our definition) fluxes. Relatively low values of
 463 Q_{nadv} were caused either by very low solar radiation and/or decreases in daily air temperatures.
 464 Regarding the main drivers of nighttime stream temperature variations, our results showed that
 465 air-water interface heat fluxes were the most important explanatory variable with R^2 ranging
 466 between 0.32 and 0.45 and between 0.16 and 0.47 in GC and BB, respectively (Fig. 12a). R^2
 467 varied spatially according to a clear spatial pattern where upward trends alternated to sudden but
 468 significant drops. Conversely, the other explanatory variables considered including discharge
 469 (Fig. 12b), average overnight stream temperature, and bed fluxes (conduction + friction) showed
 470 low correlation with overnight stream temperature variations ($R^2 < 0.16$, < 0.15 and < 0.21
 471 respectively).



472
 473 Fig. 11. Time lag [hours] distributions and boxplots between stream temperature and non-
 474 advective fluxes (a, c) and air temperature (b, d) in GC and BB.
 475

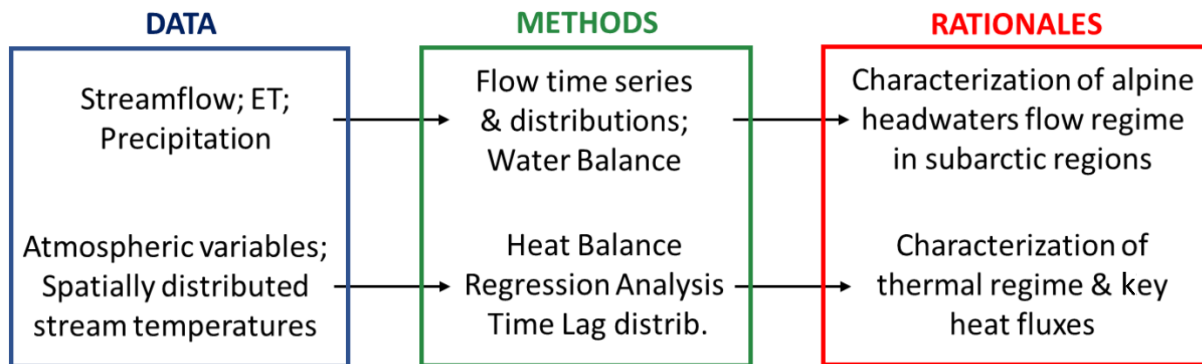


476

477 Fig. 12. Coefficient of determination (R^2) between overnight stream (ΔT_s) and air (ΔT_a)
 478 temperature variations (a); ΔT_s and specific discharge (q) (b) at the temperature monitoring
 479 sections in GC and BB. X axis indicates the distance from the upstream cross-section.

480 **5 DISCUSSION**

481 Stream temperature is the result of complex interactions between hydrological and thermal
 482 processes (Briggs *et al.*, 2018; Caissie, 2006; Vliet *et al.*, 2011). An empirical approach, based
 483 on high-resolution observations, was applied to provide insight on the hydrological and thermal
 484 regimes of two streams in adjacent permafrost influenced alpine headwater catchments (Fig. 13).



485
 486
 487

Fig. 13. Flow chart reporting data, methods and rationales of the study.

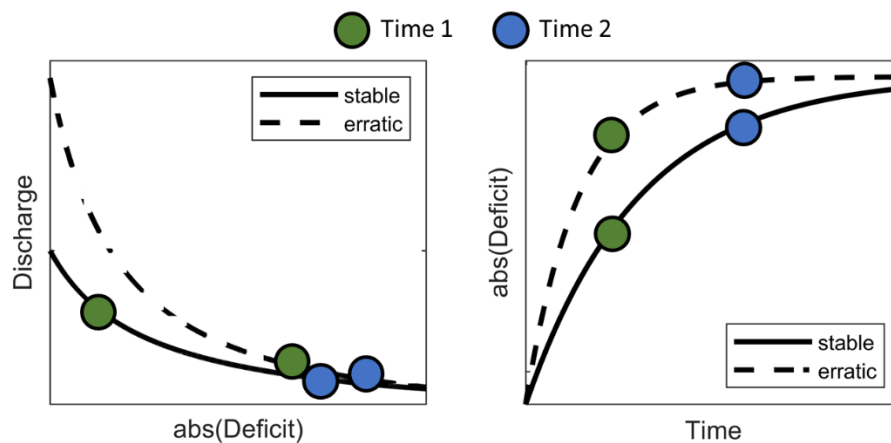
488 **5.1 Hydrology of alpine headwater catchments**

489 The two sites investigated had similar morphology, landscape, and exposure to climatic
490 conditions. However, although they were characterized by similar mean specific discharge and
491 correlated temporal flow patterns, the sites exhibited important differences. The flow regime in
492 GC was more responsive to climatic variability and more exposed to extreme weather events
493 (both peaks and troughs) than in BB. This could be due to a denser drainage network in GC, with
494 several ephemeral tributaries activated during wet periods, that facilitates connectivity between
495 hillslopes and the stream, reducing water residence time and limiting the buffering effects of
496 catchment on snowmelt/precipitation signals (Hrachowitz, Soulsby, Imholt, Malcolm & Tetzlaff,
497 2010). Average summer specific discharge in GC and BB was more than three times higher than
498 at the WCRB outlet (0.51 mm d^{-1}), as upland areas within WCRB are generally characterized by
499 higher precipitation (approximately between 25 and 35 %) and less evapotranspiration than
500 lower elevations (Pomeroy *et al.*, 1998).

501 Both sites showed a daily and sub-daily flow response typical of headwater catchments, with
502 short steep peaks alternating with more persistent low baseflow (Kosugi, Fujimoto, Katsura,
503 Kato, Sando & Mizuyama, 2011; Penna, Meerveld, Zuecco, Fontana & Borga, 2016). Peaking
504 times were generally synchronized, with random (evenly distributed between GC and BB) delays
505 not greater than 1 h. Seasonal response was typical of alpine catchments dominated by
506 permafrost at high latitudes, with the wettest period in late-spring/early-summer when most
507 snowmelt occurs (Yang, Marsh & Ge, 2014; Ye, Yang, Zhang & Kane, 2009). Note that these
508 observations occurred post-freshet when the streams were ice-free and full seasonal flows are
509 reported in Shatilla and Carey (2019).

510 In northwest Canada, global warming has been identified as the main factor responsible for the
511 positive annual and seasonal trends in air temperature between 1950 and 2012 (annual air
512 temperature $> 1.5 - 3$ °C), trends that are likely to continue or accelerate in coming decades
513 (Debeer *et al.*, 2016). According to predictions, an average increase in spring/summer air
514 temperature between 2 to 3 °C is expected in the next 60 years (Debeer *et al.*, 2016). In
515 catchments where permafrost and frozen ground are important, such as GC and BB, baseflow in
516 the dry summer period is largely driven by snowmelt processes (see high water deficit, Fig. 3)
517 and is thus very sensitive to air temperature perturbations (Huntington & Niswonger, 2012). The
518 increase in air temperature will hasten snowmelt, potentially leading to greater water deficits and
519 lower flows later in the season. Counterintuitively, we believe that the more stable BB will be
520 less hydrologically resilient to multi-decadal climate warming than GC, although the latter is
521 more hydrologically responsive on diel and seasonal timescales. Fig. 14 shows a qualitative
522 relationship between discharge and water deficit and how water deficit varies in time for a more
523 hydrologically stable (e.g. BB) and a more responsive (e.g. GC) stream in a dry period with
524 negligible precipitation. At first, under wet conditions, the erratic stream (dashed line) drains
525 much faster than the stable stream (solid line). This will lead (in the erratic stream) to a more
526 rapid increase in deficit and a substantial decrease in discharge. At a certain point the pattern
527 would be inverted; discharge will become higher in the stable stream where the deficit will now
528 start to increase more rapidly (green dots, current dry situation). At this stage, assuming an
529 extended dry period, we expect a more rapid increase in water deficit and thus a greater
530 reduction in flow in the stable stream (BB) rather than in the erratic one (GC) (blue dots,
531 extended dry period due to early snowmelt). This is in agreement with what was found by Botter
532 *et al.* (2013), who analytically demonstrated how streams characterized by unstable flow regimes

533 with enhanced intra-seasonal streamflow variability are likely to be more resilient to long-term
 534 climatic variations. Changes in precipitation (both snow and rain) as a result of global warming
 535 are also expected (Debeer *et al.*, 2016), and can either enhance or mitigate these effects.
 536 However, predictions at a local scale are highly variable (both in space and time), and thus
 537 difficult to quantify with confidence (Bates, Kundzewicz, Wu & Palutikof, 2008; Debeer *et al.*,
 538 2016). Furthermore, in alpine permafrost catchments, the increase in precipitation can hardly
 539 compensate the effect of an early snowmelt (Huntington & Niswonger, 2012), although in some
 540 recent years the importance of rainfall events to sustain late summer flow both in GC and BB has
 541 increased (Shatilla & Carey, 2019).



542 Fig. 14. Qualitative relation between discharge and deficit (left) and the variation of deficit in
 543 time (right), considering no precipitation, for two streams with contrasting responses, stable
 544 (solid line) and erratic (dashed line). Green and blue dots indicate values at an early and late
 545 time, respectively.
 546
 547

548 **5.2 Non-advective fluxes in alpine streams**

549 In agreement with previous studies located in headwater catchments, net radiation (shortwave +
 550 longwave) was the flux providing most of the daily energy inputs (Moore, Spittlehouse & Story,
 551 2005a; Moore *et al.*, 2005b; Webb & Zhang, 1997). The average proportion of approximately 60 %
 552 net radiation was in agreement with that found in Hebert *et al.* (2011), but lower than the >70 %

553 found in other studies (e.g. Khamis *et al.*, 2015). A simple explanation is that most of those studies
554 were set above the treeline (e.g. Khamis *et al.*, 2015) or subjected to bank clearcut (e.g. Moore *et*
555 *al.*, 2005b), and thus had no significant shortwave reduction due to riparian vegetation shading
556 (Garner *et al.*, 2017). Net radiation was mainly driven by shortwave radiation, while long-wave
557 radiation was relatively negligible as incoming and emitted radiation tended to be of similar
558 magnitude but opposite sign. This contrasts with what was found in the Kuparuk River (Alaska)
559 where net long wave radiation was overall an important energy sink (King *et al.*, 2016).

560 Daily energy inputs with proportions of net radiation above 50 % in the early and middle part of
561 the summer indicates that shortwave radiation remained the main positive contribution even on
562 cloudy days (Khamis *et al.*, 2015). In late summer, when daylight hours were reduced and
563 discharge started to increase, the energy contributions of shortwave radiation and (potential) bed
564 friction (~20 %) became comparable. As other studies in upland reaches suggested, the friction
565 flux was a significant energy source both in GC and BB, with percentages between the 15.8 % (on
566 average) estimated in 17 sites in the UK (Webb & Zhang, 1997; Webb *et al.*, 2008) and the 30 %
567 estimated in a headwater stream in Alaska (Chikita, Kaminaga, Kudo & Kim, 2010). In agreement
568 with some previous studies, latent heat was the main cooling process in both stream reaches (Evans
569 *et al.*, 1998; Hannah, Malcolm, Soulsby & Youngson, 2008; Hebert *et al.*, 2011), with its
570 contribution being positive only for a few days during the warmest period (around 5 July). As
571 reported by Khamis *et al.* (2015), sensible heat was overall an important energy source (~14 % on
572 average), as air temperature was generally higher than stream temperature. In general, bed
573 conduction had a buffering effect on diel and seasonal stream temperature peaks and troughs. As
574 in Webb and Zhang (1997) and Evans *et al.* (1998), bed conduction was an important heat sink,

575 accounting for 30 % and 10 % of negative non-advective fluxes in GC and BB respectively, but a
576 negligible source.

577 In alpine environments, change in vegetation type and distribution have been associated with
578 recent global warming (Danby, Koh, Hik & Price, 2011; Grabherr, Gottfried & Pauli, 2010; Post
579 *et al.*, 2009). In a study in the southwest Yukon Territory, Danby *et al.* (2011) concluded that in
580 the last four decades, an increase in air temperature has led to an increase in shrub density. This
581 suggests that in relatively narrow alpine headwaters such as GC and BB (width <3 m), with
582 shortwave radiation dominating the non-advective fluxes, a change in vegetation (increase in
583 density and height) could potentially buffer climate change effects on stream temperature (Moore
584 *et al.*, 2005a, 2005b).

585 ***5.3 Thermal regimes in alpine headwater catchments***

586 In both study reaches, our observations showed that stream temperature was very responsive to
587 changes in diel climate conditions (see Fig. S1). Stream temperature showed high variability
588 both in space and time, typical of low thermal capacity headwater streams during the summer
589 season (Dick, Tetzlaff & Soulsby, 2015). Despite differences in magnitude, stream temperature
590 variability between reaches and sections within the same reach was highly correlated ($r > 0.7$).
591 Stream temperature in BB was generally characterized by less variability (daily and sub-daily)
592 than in GC. This is probably the result of a greater groundwater/discharge flow ratio (within the
593 reach investigated), that could more effectively buffer non-advective flux troughs and peaks
594 (Brown & Hannah, 2008; Dick *et al.*, 2015; Johnson, Wilby & Toone, 2014; Snyder, Hitt &
595 Young, 2015). Daily stream temperature typically peaked later in GC than in BB, suggesting that
596 higher non-advective fluxes (as defined in section 3.2.2) are needed in BB to compensate for the
597 negative contribution of advective fluxes and maintain an overall positive energy budget.

598 Regression analysis indicated that, in both sites (slope 0.36 and 0.28, and intercept 2.00 and
599 3.03 °C in GC and BB, respectively), summer stream temperature was less sensitive to
600 atmospheric conditions than in most of the 92 sites investigated in the western part of the US
601 (mean slope and intercept 0.45 and 0.74 °C) (Mayer, 2012). Nevertheless, caution is needed in
602 this type of comparisons as, at sub-annual time scales, the sensitivity of stream temperature to air
603 temperature may strongly be affected by the presence of clouds and the non-linear relationship
604 between air and stream temperatures at low (close to 0 °C) and high stream temperatures (Luce
605 et al., 2014). Notwithstanding, the use of weekly (instead of daily) data in Mayer (2012)
606 provided conservative results. In fact, as reported in Caissie (2006), different time scales yield
607 different air/stream temperature relationships: as the time scale increase (daily, weekly, monthly
608 and annually), slopes increase, and intercepts decrease.

609 Average stream temperature for the July – August period was about 4 °C lower than average
610 stream temperature measured at the WCRB outlet (9.8 °C) for the same period, and 10 °C lower
611 than the long-term (1975 - 2010) summer average measured near the Yukon River outlet (Yang
612 *et al.*, 2014). Although comparing annual and long-term averages might not be strictly
613 appropriate, the substantial increase in temperature between headwaters and large rivers
614 demonstrates the dominance of warming with respect to cooling processes during the summer
615 season. In agreement with other studies, this indicates the importance of small tributaries to
616 sustain biodiversification in large rivers by providing temperature discontinuities (Kiffney,
617 Greene, Hall & Davies, 2006; Brown & Hannah, 2008; Johnson *et al.*, 2014). It also affirms the
618 potential importance of alpine rivers for providing future cold-water climate refugia to sustain
619 cold-water species in the context of climate warming and future heat waves (Isaak *et al.*, 2015).

620 In GC, average overnight stream temperature tended to increase along the reach, ranging from
621 0.9 to 6.9 °C and 2.5 to 7.3 °C upstream and downstream, respectively. Conversely, in BB we
622 saw a reduction of the range from 2.1 to 7.4 °C (upstream) and 2.9 to 6.7 °C (downstream) along
623 the reach. The high correlation between overnight variations in air and water temperature
624 suggests that each responded to the same temporal fluctuations in atmospheric inputs and thus
625 that air-water interface processes are the dominant factors driving nighttime stream temperature
626 (Johnson, 2004). The relationship was not constant in space but followed a cyclical pattern. This
627 consisted of a sequence of upward trends, as the time of exposure of water to atmospheric factors
628 increased along the stream, separated by sudden drops, likely due to localized surface
629 (tributaries) and subsurface flows (preferential flow paths). Magnusson, Jonas and Kirchner
630 (2012) investigated the sensitivity of overnight stream temperature variations to several
631 explanatory variables in an alpine Swiss basin and found no significant relation between surface
632 heat fluxes and overnight stream temperature dynamics. In their study, the head difference
633 between channel and groundwater was identified as the most significant explanatory variable
634 (not included in our study).

635 In the last two decades, the increase of stream temperature as a result of climate change, and its
636 consequences on river ecosystems have been well documented (e.g. Isaak *et al.*, 2012). In
637 addition, it has been shown that climate change effects on stream temperature in alpine
638 headwaters where snowmelt is an important water source, are mainly driven by hydrological
639 shifts in response to earlier onset of spring snowmelt (MacDonald *et al.*, 2014), a trend projected
640 to continue in the future (Stewart, Morgenstern & McDonnell, 2010). Our results suggest that,
641 due to its more stable and resilient thermal regime, BB will be less affected by direct climate
642 change effects. The relatively high contribution of groundwater, generally with opposite sign

643 with respect to net non-advective fluxes, can effectively buffer extreme climatic conditions. This
644 occurs as groundwater input tends to moderate both temperature peaks and troughs, but its ability
645 to attenuate future low frequency warming may be impacted by future aquifer warming (Kurylyk
646 *et al.*, 2014). However, in permafrost sites, discharging groundwater may stay cool in a warmer
647 climate as it continues to thermally interact with ground ice. Nonetheless, BB seems to be more
648 exposed to indirect effects, as in BB a greater reduction in discharge and thus in thermal capacity
649 is expected (section 5.1). In conclusion, we believe long-term studies, meaning long-term
650 hydrologic and atmospheric data, are necessary in order to make reliable long-term predictions
651 accounting for global warming, given the complexity of the thermal and hydrological processes
652 involved.

653 ***5.4 Study limitations***

654 The uncertainty associated with measuring instruments was deemed negligible compared to the
655 magnitude of the variations in space and time considered and did not significantly impact our
656 results. In some specific occasions, small-scale spatial variability in atmospheric conditions and
657 localized rainfall events may not have been well captured by a single weather station. A critical
658 analysis of the data helped to identify such events. For example, on 9 July a major flood was
659 recorded in GC (confirmed by flow measurements in upstream gauges), while precipitation and
660 flow records in BB showed only a mild event. Nevertheless, we believe that the overall
661 consistency of our results demonstrated that these errors did not impact our analysis and findings
662 significantly.

663 A further source of uncertainty is associated with errors in flow estimations, the sources of which
664 are well documented in the literature. Despite the lack of a control structure, repeated measures
665 at GC over 20 years using both dilution and velocity-area methods across a range of flow

666 indicates an error < 10%, which is similar to that reported by Hood, Roy and Hayashi (2006)
667 using the velocity-area method for several alpine streams. While we do not have long-term flows
668 from BB, similar methodology and a robust rating curve in 2016 suggests that the error in flow
669 estimates is significantly lower than the differences in specific flows for the two streams.

670 As a single weather station was utilized, it was not possible to account for small-scale variability
671 in some of the atmospheric variables. It is important to note, however, that many stream
672 temperature studies have relied on meteorological stations several kilometers away, especially
673 for streams that are logistically difficult to reach (Hebert et al., 2011). The most affected
674 atmospheric variables include wind speed and humidity, for which we could not account for
675 riparian vegetation effects. This might result in estimating potential (maximum in absolute
676 terms) Φ_{lat} and Φ_{sens} rather than actual values.

677 Another important limitation that future studies should try to overcome is related to the timespan
678 considered. The study provided useful insights on the thermal response of streams to hydrologic
679 and atmospheric processes; however a short-term study such as ours cannot be confidently
680 employed to identify any long-term trend or assess climate change impacts (Bolduc &
681 Lamoureux, 2018), revealing the importance of long-term hydrologic and thermal monitoring
682 (e.g. Rasouli *et al.*, 2019).

683 Furthermore, our study is limited to the summer season as it was logistically difficult to collect
684 observations during the colder period of the year. This study period is common among stream
685 temperature studies set in remote regions with challenging climatic conditions such as ours, often
686 preventing a full characterization of the hydrological and thermal cycles across seasons. Thus, to
687 fill this gap, future studies should attempt to include winter stream thermal regimes, as these
688 have been shown to also be important for aquatic habitat (e.g., Cunjak & Power, 1986).

689 **5.5 Conclusions and future directions**

690 The present study provided insights on the processes governing the hydrologic and thermal
691 regimes in two adjacent subarctic alpine headwaters. This is important as alpine headwaters in
692 permafrost regions have been shown to be among the most sensitive environments to climate
693 change. Our results highlighted the major role played by groundwater on the hydrologic and
694 thermal response of sub-alpine headwater catchments. A high groundwater/discharge ratio could
695 effectively moderate both flow and stream temperature extremes. Overall, in both streams, solar
696 radiation and latent heat were respectively the most important heat source and sink.

697 The last decade has seen a reduction of experimental long-term data collection (Tetzlaff, Carey,
698 McNamara, Laudon & Soulsby, 2017). In this regard, we want to highlight the importance that
699 ongoing collection of field data has on supporting both empirical and model-based studies. In
700 addition, in headwater catchments at high latitudes or elevations, long-term and spatially
701 distributed studies are extremely rare (e.g. Bolduc and Lamoureux, 2018). Therefore, we believe
702 that in future studies, long-term data sets (in alpine headwater catchments) in combination with
703 models should be used to: (1) identify significant long-term trends; (2) quantify the potential
704 effects of changing climate and land use (e.g. change in vegetation related to global warming) on
705 flow and thermal regimes; and (3) provide specific tools to assist catchment managers to evaluate
706 and apply suitable management strategies.

707

708 **References**

709 Arora R, Tockner K, Venohr M. 2016. Changing river temperatures in northern Germany:

710 Trends and drivers of change. *Hydrological Processes* **30**: 3084–3096 DOI:

711 10.1002/hyp.10849

Flow and thermal regimes in subarctic headwaters

- 712 Baldocchi DD, Hincks BB, Meyers TP. 1988. Measuring Biosphere-Atmosphere Exchanges of
713 Biologically Related Gases with Micrometeorological Methods. *Ecology* **69** (5): 1331–1340
714 DOI: 10.2307/1941631
- 715 Bates BC, Kundzewicz ZW, Wu S, Palutikof JP. 2008. *Climate Change and Water. Technical*
716 *Paper of the Intergovernmental Panel on Climate Change (IPCC)*. DOI:
717 10.1016/j.jmb.2010.08.039
- 718 Bolduc C, Lamoureux SF. 2018. Multiyear variations in High Arctic river temperatures in
719 response to climate variability. *Arctic Science* **4** (4): 605–623 DOI: 10.1139/as-2017-0053
- 720 Botter G, Basso S, Rodriguez-Iturbe I, Rinaldo A. 2013. Resilience of river flow regimes.
721 *Proceedings of the National Academy of Sciences* DOI: 10.1073/pnas.1311920110
- 722 Bourque CP-A, Pomeroy JH. 2001. Effects of forest harvesting on summer stream temperatures
723 in New Brunswick, Canada: an inter-catchment, multiple-year comparison. *Hydrology and*
724 *Earth System Sciences* DOI: 10.5194/hess-5-599-2001
- 725 Briggs MA, Johnson ZC, Snyder CD, Hitt NP, Kurylyk BL, Lautz L, Irvine DJ, Hurley ST, Lane
726 JW. 2018. Inferring watershed hydraulics and cold-water habitat persistence using multi-
727 year air and stream temperature signals. *Science of the Total Environment* DOI:
728 10.1016/j.scitotenv.2018.04.344
- 729 Broadmeadow SB, Jones JG, Langford TEL, Shaw PJ, Nisbet TR. 2011. The influence of
730 riparian shade on lowland stream water temperatures in southern England and their viability
731 for brown trout. *River Research and Applications* **27** (2): 226–237 DOI: 10.1002/rra.1354
- 732 Brown LE, Hannah DM. 2008. Spatial heterogeneity of water temperature across an alpine river
733 basin. *Hydrological Processes* DOI: 10.1002/hyp.6982

Flow and thermal regimes in subarctic headwaters

- 734 Brown LE, Hannah DM, Milner AM. 2005. Spatial and temporal water column and streambed
735 temperature dynamics within an alpine catchment: Implications for benthic communities.
736 *Hydrological Processes* **19**: 1585–1610 DOI: 10.1002/hyp.5590
- 737 Caissie D. 2006. The thermal regime of rivers: a review. *Freshwater Biology* **51** (8): 1389–1406
738 DOI: 10.1111/j.1365-2427.2006.01597.x
- 739 Caissie D, Luce CH. 2017. Quantifying streambed advection and conduction heat fluxes. *Water*
740 *Resources Research* DOI: 10.1002/2016WR019813
- 741 Carey SK, Quinton WL. 2005. Evaluating runoff generation during summer using hydrometric ,
742 stable isotope and hydrochemical methods in a discontinuous permafrost. **114** (October
743 2004): 95–114 DOI: 10.1002/hyp.5764
- 744 Carey SK, Boucher JL, Duarte CM. 2013. Inferring groundwater contributions and pathways to
745 streamflow during snowmelt over multiple years in a discontinuous permafrost subarctic
746 environment (Yukon, Canada). *Hydrogeology Journal* **21**: 67–77 DOI: 10.1007/s10040-
747 012-0920-9
- 748 Chikita KA, Kaminaga RYO, Kudo I, Kim Y. 2010. PARAMETERS DETERMINING WATER
749 TEMPERATURE OF A PROGLACIAL STREAM : THE PHELAN CREEK AND THE
750 GULKANA GLACIER , ALASKA. **1004** (September 2009): 995–1004 DOI: 10.1002/rra
- 751 Cunjak RA, Power G (1986) Winter habitat utilization by stream resident brook trout (*Salvelinus*
752 *fontinalis*) and brown trout (*Salmo trutta*). *Can J Fish Aquat Sci* 43:1970–1981
- 753 Danby RK, Koh S, Hik DS, Price LW. 2011. Four Decades of Plant Community Change in the
754 Alpine Tundra of Southwest Yukon , Canada: 660–671 DOI: 10.1007/s13280-011-0172-2
- 755 Debeer CM, Wheater HS, Carey SK, Chun KP. 2016. Recent climatic , cryospheric , and

Flow and thermal regimes in subarctic headwaters

- 756 hydrological changes over the interior of western Canada : a review and synthesis: 1573–
757 1598 DOI: 10.5194/hess-20-1573-2016
- 758 Dick JJ, Tetzlaff D, Soulsby C. 2015. Landscape influence on small-scale water temperature
759 variations in a moorland catchment. *Hydrological Processes* **29** (14): 3098–3111 DOI:
760 10.1002/hyp.10423
- 761 Docherty C, Docherty CL, Abermann J, Lund M, Hannah DM. 2019. Arctic river temperature
762 dynamics in a changing climate. *River Res Applic* **35** (October): 1212–1227 DOI:
763 10.1002/rra.3537
- 764 Evans EC, Petts GE. 1997. Hyporheic temperature patterns within riffles. *Hydrological Sciences*
765 *Journal* **42** (2): 199–213 DOI: 10.1080/02626669709492020
- 766 Evans EC, McGregor GR, Petts GE. 1998. River energy budgets with special reference to river
767 bed processes. *Hydrological Processes* **12** (April 1997): 575–595 DOI:
768 10.1002/(SICI)1099-1085(19980330)12:4<575::AID-HYP595>3.0.CO;2-Y
- 769 Ferrazzi M, Botter G. 2019. Contrasting signatures of distinct human water uses in regulated
770 flow regimes Contrasting signatures of distinct human water uses in regulated flow regimes.
771 *Environmental Research Communications* **1** (7): 71003 DOI: 10.1088/2515-7620/ab3324
- 772 Ficklin DL, Stewart IT, Maurer EP. 2013. Effects of climate change on stream temperature ,
773 dissolved oxygen , and sediment concentration in the Sierra Nevada in California. **49**
774 (March 2012): 2765–2782 DOI: 10.1002/wrcr.20248
- 775 Fullerton AH, Torgersen CE, Lawler JJ, Steel EA, Ebersole JL, Lee SY. 2018. Longitudinal
776 thermal heterogeneity in rivers and refugia for coldwater species: effects of scale and
777 climate change. *Aquatic Sciences* DOI: 10.1007/s00027-017-0557-9

- 778 Gaay AC De, Blokland P. 1970. The canalization of the lower Rhine. *I RIJKSWATERSTAAT*
779 *COMMUNICATIONS*
- 780 Garner G, Malcolm IA, Sadler JP, Hannah DM. 2017. The role of riparian vegetation density,
781 channel orientation and water velocity in determining river temperature dynamics. *Journal*
782 *of Hydrology* **553**: 471–485 DOI: 10.1016/J.JHYDROL.2017.03.024
- 783 Genç O, Ardiçlioğlu M, Ağırlioğlu N. 2015. Calculation of mean velocity and discharge using
784 water surface velocity in small streams, *Flow Measurement and Instrumentation*, Vol. 41, P
785 115-120, DOI: 10.1016/j.flowmeasinst.2012.05.001
- 786 Glose AM, Lautz LK, Baker EA. 2017. Stream heat budget modeling with HFLUX: Model
787 development, evaluation, and applications across contrasting sites and seasons.
788 *Environmental Modelling and Software* DOI: 10.1016/j.envsoft.2017.02.021
- 789 Gooseff MN. 2010. Defining hyporheic zones - advancing our conceptual and operational
790 definitions of where stream water and groundwater meet. *Geography Compass* **4** (8): 945–
791 955 DOI: 10.1111/j.1749-8198.2010.00364.x
- 792 Grabherr G, Gottfried M, Pauli H. 2010. Climate Change Impacts in Alpine Environments.
793 *Geography Compass* **4** (8): 1133–1153 DOI: 10.1111/j.1749-8198.2010.00356.x
- 794 Hannah DM, Garner G. 2015. River water temperature in the United Kingdom: Changes over the
795 20th century and possible changes over the 21st century. *Progress in Physical Geography*
796 **39** (1): 68–92 DOI: 10.1177/0309133314550669
- 797 Hannah DM, Malcolm IA, Soulsby C, Youngson AF. 2008. A comparison of forest and
798 moorland stream microclimate, heat exchanges and thermal dynamics. *Hydrological*
799 *Processes* **22** (7): 919–940 DOI: 10.1002/hyp.7003

Flow and thermal regimes in subarctic headwaters

- 800 Hari R., Livingstone DM, Siber R, Burkhardt-Holm P, Guttinger H. 2006. Consequences of
801 climatic change for water temperature and brown trout populations in Alpine rivers and
802 streams. *Global Change Biology* **12**: 10–26 DOI: 10.1111/j.1365-2486.2005.01051.x
- 803 Harrington JS, Kurylyk BL. 2017. Influence of a rock glacier spring on the stream energy budget
804 and cold - water refuge in an alpine stream. *Hydrological Processes* (April): 4719–4733
805 DOI: 10.1002/hyp.11391
- 806 Hebert C, Caissie D, Satish MG, El-jabi N. 2011. Study of stream temperature dynamics and
807 corresponding heat fluxes within Miramichi River catchments (New Brunswick , Canada).
808 **2455** (March): 2439–2455 DOI: 10.1002/hyp.8021
- 809 Hood, J. L., Roy, J. W., & Hayashi, M. (2006). Importance of groundwater in the water balance
810 of an alpine headwater lake. *Geophysical Research Letters*, 33(L13405), 1–5.
- 811 Hrachowitz M, Soulsby C, Imholt C, Malcolm IA, Tetzlaff D. 2010. Thermal regimes in a large
812 upland salmon river: A simple model to identify the influence of landscape controls and
813 climate change on maximum temperatures. *Hydrological Processes* DOI: 10.1002/hyp.7756
- 814 Huntington JL, Niswonger RG. 2012. Role of surface-water and groundwater interactions on
815 projected summertime streamflow in snow dominated regions : An integrated modeling
816 approach. **48**: 1–20 DOI: 10.1029/2012WR012319
- 817 Isaak DJ, Wollrab S, Horan D, Chandler G. 2012. Climate change effects on stream and river
818 temperatures across the northwest U.S. from 1980–2009 and implications for salmonid
819 fishes. *Climatic Change* **113** (2): 499–524 DOI: 10.1007/s10584-011-0326-z
- 820 Isaak DJ, Young MK, Luce CH, Hostetler SW, Wenger SJ, Peterson EE, Ver Hoef JM, Groce
821 MC, Horan DL, Nagel DE. 2016. Slow climate velocities of mountain streams portend their

Flow and thermal regimes in subarctic headwaters

- 822 role as refugia for cold-water biodiversity. *Proceedings of the National Academy of*
823 *Sciences of the United States of America* DOI: 10.1073/pnas.1522429113
- 824 Isaak DJ, Young MK, Nagel DE, Horan DL, Groce MC. 2015. The cold-water climate shield:
825 delineating refugia for preserving salmonid fishes through the 21st century. *Global Change*
826 *Biology* **21** (7): 2540–2553 DOI: 10.1111/gcb.12879
- 827 Johnson MF, Wilby RL, Toone JA. 2014. Inferring air-water temperature relationships from
828 river and catchment properties. *Hydrological Processes* **28** (6): 2912–2928 DOI:
829 10.1002/hyp.9842
- 830 Johnson SL. 2004. Factors influencing stream temperatures in small streams: substrate effects
831 and a shading experiment. *Canadian Journal of Fisheries and Aquatic Sciences* **61** (6):
832 913–923 DOI: 10.1139/f04-040
- 833 Kaandorp VP, Doornenbal PJ, Kooi H, Peter Broers H, de Louw PGB. 2019. Temperature
834 buffering by groundwater in ecologically valuable lowland streams under current and future
835 climate conditions. *Journal of Hydrology X* DOI: 10.1016/j.hydroa.2019.100031
- 836 Kelleher C, Wagener T, Gooseff M, Mcglynn B, Mcguire K, Marshall L. 2012. Investigating
837 controls on the thermal sensitivity of Pennsylvania streams. *Hydrological Processes* **26**:
838 771–785 DOI: 10.1002/hyp.8186
- 839 Khamis K, Brown LE, Milner AM, Hannah DM. 2015. Heat exchange processes and thermal
840 dynamics of a glacier-fed alpine stream. *Hydrological Processes* **3317** (March): 3306–3317
841 DOI: 10.1002/hyp.10433
- 842 Kiffney PM, Greene CM, Hall JE, Davies JR. 2006. Tributary streams create spatial
843 discontinuities in habitat , biological productivity , and diversity in mainstem rivers.

- 844 *Canadian Journal of Fisheries and Aquatic Sciences* **2530**: 2518–2530 DOI: 10.1139/F06-
845 138
- 846 King T V., Neilson BT. 2019. Quantifying Reach-Average Effects of Hyporheic Exchange on
847 Arctic River Temperatures in an Area of Continuous Permafrost. *Water Resources Research*
848 DOI: 10.1029/2018WR023463
- 849 King T V., Neilson BT, Overbeck LD, Kane DL. 2016. Water temperature controls in low arctic
850 rivers. *Water Resources Research* DOI: 10.1002/2015WR017965
- 851 Kinouchi T, Yagi H, Miyamoto M. 2007. Increase in stream temperature related to
852 anthropogenic heat input from urban wastewater. *Journal of Hydrology* **335** (1–2): 78–88
853 DOI: 10.1016/j.jhydrol.2006.11.002
- 854 Kosugi K, Fujimoto M, Katsura S, Kato H, Sando Y, Mizuyama T. 2011. Localized bedrock
855 aquifer distribution explains discharge from a headwater catchment. *Water Resources*
856 *Research* **47**: 1–16 DOI: 10.1029/2010WR009884
- 857 Kurylyk BL, Macquarrie KTB, Linnansaari T, Cunjak RA, Curry RA. 2015. Preserving,
858 augmenting, and creating cold-water thermal refugia in rivers: Concepts derived from
859 research on the Miramichi River, New Brunswick (Canada). *Ecohydrology* DOI:
860 10.1002/eco.1566
- 861 Kurylyk BL, MacQuarrie KTB, Voss CI. 2014. Climate change impacts on the temperature and
862 magnitude of groundwater discharge from shallow, unconfined aquifers. *Water Resources*
863 *Research* DOI: 10.1002/2013WR014588
- 864 Kurylyk BL, Moore RD, Macquarrie KTB. 2016. Scientific briefing: Quantifying streambed heat
865 advection associated with groundwater-surface water interactions. *Hydrological Processes*

866 DOI: 10.1002/hyp.10709

867 Le Coz J, Camenen B, Peyrard X, Dramais G. 2012. Uncertainty in open-channel discharges
868 measured with the velocity–area method, *Flow Measurement and Instrumentation*, Vol. 26,
869 P 18-29, DOI: 10.1016/j.flowmeasinst.2012.05.001

870 Leach JA, Moore RD. 2010. Above-stream microclimate and stream surface energy exchanges in
871 a wildfire-disturbed riparian zone. *Hydrological Processes* DOI: 10.1002/hyp.7639

872 Leach JA, Moore RD. 2014. Winter stream temperature in the rain-on-snow zone of the Pacific
873 Northwest: Influences of hillslope runoff and transient snow cover. *Hydrology and Earth
874 System Sciences* DOI: 10.5194/hess-18-819-2014

875 Leach JA, Moore RD. 2017. Insights on stream temperature processes through development of a
876 coupled hydrologic and stream temperature model for forested coastal headwater
877 catchments. *Hydrological Processes* DOI: 10.1002/hyp.11190

878 Lewkowitz AG, Ednie M. 2004. Probability mapping of mountain permafrost using the BTS
879 method, Wolf Creek, Yukon Territory, Canada. *Permafrost and Periglacial Processes* **15**:
880 67–80 DOI: 10.1002/ppp.480

881 Lisi PJ, Schindler DE, Cline TJ, Scheuerell MD, Walsh PB. 2015. Watershed geomorphology
882 and snowmelt control stream thermal sensitivity to air temperature. *Geophysical Research
883 Letters* **42** (9): 3380–3388 DOI: 10.1002/2015GL064083

884 Liu B, Yang D, Ye B, Berezovskaya S. 2005. Long-term open-water season stream temperature
885 variations and changes over Lena River Basin in Siberia. *Global and Planetary Change* **48**:
886 96–111 DOI: 10.1016/j.gloplacha.2004.12.007

887 Luce C, Staab B, Kramer M, Wenger S, Isaak D, McConnell C. 2014. Sensitivity of summer

Flow and thermal regimes in subarctic headwaters

- 888 stream temperatures to climate variability in the Pacific Northwest. *Water Resources*
889 *Research* DOI: 10.1002/2013WR014329
- 890 Macdonald RJ, Boon S, Byrne JM, Silins U. 2014. A comparison of surface and subsurface
891 controls on summer temperature in a headwater stream. *Hydrological Processes* **2347** (April
892 2013): 2338–2347 DOI: 10.1002/hyp.9756
- 893 MacDonald RJ, Boon S, Byrne JM, Robinson MD, Rasmussen JB. 2014. Potential future climate
894 effects on mountain hydrology, stream temperature, and native salmonid life-history.
895 *Canadian Journal of Fisheries and Aquatic Sciences* **71** (October 2013): 189–202 DOI:
896 10.1139/cjfas-2013-0221
- 897 Magnusson J, Jonas T, Kirchner JW. 2012. Temperature dynamics of a proglacial stream :
898 Identifying dominant energy balance components and inferring spatially integrated
899 hydraulic geometry. **48**: 1–16 DOI: 10.1029/2011WR011378
- 900 Marine KR, Cech JJ. 2004. Effects of High Water Temperature on Growth, Smoltification , and
901 Predator Avoidance in Juvenile Sacramento River Chinook Salmon. *North American*
902 *Journal of Fisheries Management* **5947** (24): 198–210 DOI: 10.1577/M02-142
- 903 Mayer TD. 2012. Controls of summer stream temperature in the Pacific Northwest. *Journal of*
904 *Hydrology* **475**: 323–335 DOI: 10.1016/j.jhydrol.2012.10.012
- 905 McDowell RW, Elkin KR, Kleinman PJA. 2017. Temperature and Nitrogen Effects on
906 Phosphorus Uptake by Agricultural Stream-Bed Sediments: 295–301 DOI:
907 10.2134/jeq2016.09.0352
- 908 Moore RD, Spittlehouse DL, Story A. 2005a. Riparian microclimate and stream temperature
909 response to forest harvesting: A review. *Journal Of The American Water Resources*

- 910 *Association* **7** (4): 813–834 DOI: 10.1111/j.1752-1688.2005.tb04465.x
- 911 Moore RD, Sutherland P, Gomi T, Dhakal A. 2005b. Thermal regime of a headwater stream
912 within a clear-cut , coastal British Columbia , Canada. *Hydrological Processes* **2608** (July
913 2004): 2591–2608 DOI: 10.1002/hyp.5733
- 914 Mougeot C, Smith C. 1994. Soil Survey of the Whitehorse Area. *Takhini Valley. Research*
915 *Branch, Agriculture and Agri-food Canada. Whitehorse. 1*
- 916 Okkonen J, Jyrkama M, Kløve B. 2010. A conceptual approach for assessing the impact of
917 climate change on groundwater and related surface waters in cold regions (Finland).
918 *Hydrogeology Journal* **18**: 429–439 DOI: 10.1007/s10040-009-0529-9
- 919 Pekarova P, Halmova D, Miklanek P, Onderka M, Pekar J, Skoda P. 2008. Is the Water
920 Temperature of the Danube River at Bratislava, Slovakia, Rising? *Journal of*
921 *Hydrometeorology* **9** (5): 1115–1122 DOI: 10.1175/2008JHM948.1
- 922 Penna D, Meerveld HJ Van, Zuecco G, Fontana GD, Borga M. 2016. Hydrological response of
923 an Alpine catchment to rainfall and snowmelt events. *JOURNAL OF HYDROLOGY* **537**:
924 382–397 DOI: 10.1016/j.jhydrol.2016.03.040
- 925 Pepin N, Bradley RS, Diaz HF, Baraer M, Caceres EB, Forsythe N, Fowler H, Greenwood G,
926 Hashmi MZ, Liu XD, et al. 2015. Elevation-dependent warming in mountain regions of the
927 world. *Nature Climate Change* **5**: 424–430 DOI: 10.1038/nclimate2563
- 928 Pomeroy J, Hedstrom N, Parviainen J. 1998. The Snow Mass Balance of Wolf Creek , Yukon :
929 Effects of Snow Sublimation and Redistribution. (March)
- 930 Poole GC, Berman CH. 2001. An Ecological Perspective on In-Stream Temperature: Natural
931 Heat Dynamics and Mechanisms of Human-Caused Thermal Degradation. *Environmental*

- 932 *Management* **27** (6): 787–802 DOI: 10.1007/s002670010188
- 933 Poole GC, O’Daniel SJ, Jones KL, Woessner WW, Bernhardt ES, Helton AM, Stanford JA, Boer
934 BR, Beechie TJ. 2008. Hydrologic Spiralling : The Role of Multiple Interactive Flow Paths
935 in Stream Ecosystems. *River Research and Application* **24**: 1018–1031 DOI:
936 10.1002/rra.1099
- 937 Post E, Forchhammer MC, Bret-Harte MS, Callaghan T V, Christensen TR, Elberling B, Fox
938 AD, Gilg O, Hik DS, Høye TT, et al. 2009. Ecological Dynamics Across the Arctic
939 Associated with Recent Climate Change. *Science* **325** (5946): 1355 LP – 1358 DOI:
940 10.1126/science.1173113
- 941 Power G, Brown RS, Imhof JG. 1999. Groundwater and fish—insights from northern North
942 America. *Hydrological Processes* DOI: 10.1002/(sici)1099-1085(19990228)13:3<401::aid-
943 hyp746>3.3.co;2-1
- 944 Quinton WL, Hayashi M, Chasmer LE. 2009. Peatland hydrology of discontinuous permafrost in
945 the northwest territories: Overview and synthesis. *Canadian Water Resources Journal* **34**:
946 311–328 DOI: 10.4296/cwrj3404311
- 947 Rasouli K, Pomeroy JW, Janowicz JR, Williams TJ, Carey SK. 2019. A long-term
948 hydrometeorological dataset (1993 – 2014) of a northern mountain basin : Wolf Creek
949 Research Basin , Yukon Territory , Canada: 89–100
- 950 Seguin M, Stein J, Nilo O, Jalbert C. 1999. Hydrogeophysical Investigation of the Wolf Creek
951 Watershed , Yukon Territory , Canada. **Proc. from**: 55–78
- 952 Shatilla N, Carey S. 2019. Assessing inter-annual and seasonal patterns of DOC and DOM
953 quality across a complex alpine watershed underlain by discontinuous permafrost in Yukon,

Flow and thermal regimes in subarctic headwaters

- 954 Canada. *Hydrology and Earth System Sciences* DOI: 10.5194/hess-23-3571-2019
- 955 Snyder CD, Hitt NP, Young JA. 2015. Accounting for groundwater in stream fish thermal habitat
956 responses to climate change. *Ecological Applications* **25** (5): 1397–1419 DOI: 10.1890/14-
957 1354.1
- 958 Steel EA, Beechie TJ, Torgersen CE, Fullerton AH. 2017. Envisioning, Quantifying, and
959 Managing Thermal Regimes on River Networks. *BioScience*: 506–522 DOI:
960 10.1093/biosci/bix047
- 961 Stewart MK, Morgenstern U, McDonnell JJ. 2010. Truncation of stream residence time: how the
962 use of stable isotopes has skewed our concept of streamwater age and origin. *Hydrological*
963 *Processes* **24** (12): 1646–1659 DOI: 10.1002/hyp.7576
- 964 Tetzlaff D, Carey SK, McNamara JP, Laudon H, Soulsby C. 2017. The essential value of long-
965 term experimental data for hydrology and water management. *Water Resources Research*
966 **53** (4): 2598–2604 DOI: 10.1002/2017WR020838
- 967 Theurer FD, Voos KA, Miller WJ. 1984. No Title. Instream water temperature model. Instream
968 flow information paper 16, US Fish and Wildlife Service.
- 969 Vliet MTH Van, Ludwig F, Zwolsman JJG, Weedon GP, Kabat P. 2011. Global river
970 temperatures and sensitivity to atmospheric warming and changes in river flow. **47**
971 (February 2010) DOI: 10.1029/2010WR009198
- 972 Van Vliet MTH, Franssen WHP, Yearsley JR, Ludwig F, Haddeland I, Lettenmaier DP, Kabat P.
973 2013. Global river discharge and water temperature under climate change. *Global*
974 *Environmental Change* **23** (2): 450–464 DOI: 10.1016/j.gloenvcha.2012.11.002
- 975 Walvoord MA, Kurylyk BL. 2016. Hydrologic impacts of thawing permafrost—a review.

Flow and thermal regimes in subarctic headwaters

- 976 *Vadose Zone Journal* DOI: 10.2136/vzj2016.01.0010
- 977 Walvoord MA, Voss CI, Wellman TP. 2012. Influence of permafrost distribution on
978 groundwater flow in the context of climate-driven permafrost thaw: Example from Yukon
979 Flats Basin, Alaska, United States. *Water Resources Research* DOI:
980 10.1029/2011WR011595
- 981 Webb BW, Zhang Y. 1997. Spatial and seasonal variability in the components of the river heat
982 budget. *Hydrological Processes* **11**: 79–101 DOI: 10.1002/(SICI)1099-
983 1085(199701)11:1<79::AID-HYP404>3.3.CO;2-E
- 984 Webb BW, Hannah DM, Moore RD, Brown LE, Nobilis F. 2008. Recent advances in stream and
985 river temperature research. *Hydrological Processes* **22**: 902–918 DOI: 10.1002/hyp.6994
- 986 Yang D, Marsh P, Ge S. 2014. ScienceDirect Heat flux calculations for Mackenzie and Yukon
987 Rivers. *Polar Science* **8** (3): 232–241 DOI: 10.1016/j.polar.2014.05.001
- 988 Ye B, Yang D, Zhang Z, Kane DL. 2009. Variation of hydrological regime with permafrost
989 coverage over Lena Basin in Siberia. *J. Geophys. Res.* **114** (April) DOI:
990 10.1029/2008JD010537
- 991